Force Spectroscopy of Chromatin Fibers: Extracting Energetics and Structural Information from Monte Carlo Simulations

Nick Kepper,[1] Ramona Ettig,[1] Rene Stehr,[2] Sven Marnach,[3] Gero Wedemann,[2] Karsten Rippe[1]

[1] *Deutsches Krebsforschungszentrum and BioQuant, Research Group Genome Organization and Function, Im Neuenheimer Feld 280, 69120 Heidelberg, Germany*

[2] *University of Applied Sciences Stralsund, CC Bioinformatics, Zur Schwedenschanze 15, 18435 Stralsund, Germany*

[3] *Interdisciplinary Center for Scientific Computing, University of Heidelberg, Im Neuenheimer Feld 368, 69120 Heidelberg, Germany*

Received 14 December 2010; revised 18 January 2011; accepted 18 January 2011
Published online 3 February 2011 in Wiley Online Library (wileyonlinelibrary.com). DOI 10.1002/bip.21598

ABSTRACT:

The folding of the nucleosome chain into a chromatin fiber is a central factor for controlling the DNA access of protein factors involved in transcription, DNA replication and repair. Force spectroscopy experiments with chromatin fibers are ideally suited to dissect the interactions that drive this process, and to probe the underlying fiber conformation. However, the interpretation of the experimental data is fraught with difficulties due to the complex interplay of the nucleosome geometry and the different energy terms involved. Here, we apply a Monte Carlo simulation approach to derive virtual chromatin fiber force spectroscopy curves. In the simulations, the effect of the nucleosome geometry, repeat length, nucleosome–nucleosome interaction potential, and the unwrapping of the DNA from the histone protein core on the shape of the force-extension curves was investigated. These simulations provide a framework for the evaluation of experimental data sets. We demonstrate how the relative contributions of DNA bending and twisting, nucleosome unstacking and unwrapping the nucleosomal DNA from the histone octamer can be dissected for a given fiber geometry. © *2011 Wiley Periodicals, Inc. Biopolymers 95: 435–447, 2011.*

Keywords: chromatin structure; force spectroscopy; Monte Carlo simulation; nucleosome

This article was originally published online as an accepted preprint. The "Published Online" date corresponds to the preprint version. You can request a copy of the preprint by emailing the Biopolymers editorial office at biopolymers@wiley.com

INTRODUCTION

The DNA-binding of many protein factors involved in processes like transcription, replication, repair, and recombination depends on the chromatin organization. Both the wrapping of the DNA around the histone octamer complex as well as the folding of the nucleosome chain into a fiber can regulate the accessibility of the DNA sequence for the binding of proteins as described in a number of reviews.[1–4] A 50-fold difference in the accessibility of the linker DNA has been reported based on a comparison of dinucleosomes with folded 17mer nucleosome arrays.[5] In addition, the binding of linker histone H1 induces a further compaction of the fiber structure.[2,6] While the structure of the nucleosome is known at atomic resolution,[7] the conformation of the 30 nm fiber remains controversial, and various models have been proposed.[2,6,8–10] These include (i) a two-start fiber helix derived from the crystal structure of a tetranucleosome

Additional Supporting Information may be found in the online version of this article.

Correspondence to: Karsten Rippe; e-mail: karsten.rippe@dkfz.de

Contract grant sponsor: DFG
Contract grant number: Ri 1283/8-1
Contract grant sponsor: BMBF (Services@MediGRID)
Contract grant number: 01IG07015G
Contract grant sponsor: North German Supercomputing Alliance (HLRN)
Contract grant number: mvb00007
Contract grant sponsor: Project EpiGenSys within the EraSysBioPlus Program

particle,[11] (ii) a one-start helix with interdigitated nucleosomes based on electron microscopy studies of chromatin fibers reconstituted in vitro,[2,12] and (iii) two-start helix conformations with crossed-linker DNA and a zig-zag-like DNA backbone with a so-called nucleosome stem motif.[13,14] The fiber conformation appears to be dependent on the nucleosome repeat length (NRL),[15–17] the presence and type of linker histones,[2,6,16] the ionic conditions,[18–22] and the acetylation state of histone H4 residue lysine 16.[23,24] For the folding of the nucleosome chain into a fiber, the interactions between nucleosomes have to compensate for the unfavorable energetic terms that arise from bending/twisting of the linker DNA, the electrostatic repulsion of the linker DNA and decreased conformational entropy.[15,25,26] While the DNA-associated energetic terms are well defined from studies of free DNA, the contribution of the nucleosome–nucleosome interaction potential is not known precisely. To investigate this experimentally, force spectroscopy studies were conducted.[27–29] In these experiments, a nucleosome chain is bound at one end to a solid support and is then extended by pulling at the other end using optical tweezers or an atomic force microscopy setup. The increase in distance of the two ends of the fiber at a given force in the regime from ~0.1 pN to ~40 pN is then computed as a force-distance curve. The first experiments of this type were conducted with native chromatin fibers derived from chicken erythrocytes.[28] More recently, reconstituted nucleosome arrays have been investigated in which the protein composition is better defined.[27,29–32] The values for the nucleosome–nucleosome energy derived from these experiments vary from 3.4 to 17 k_BT. Several approaches have been reported to dissect the energetic terms that govern the force-distance curve for a given type of fiber. For the description of the nucleosome chain geometry according to a two-angle model, an analytical approach was used.[33] In addition, Monte Carlo (MC) simulations of force spectroscopy experiments were conducted to evaluate the elastic properties as well as the nucleosome–nucleosome interaction potential of the chromatin fiber.[33–36]

In our recent work, we have advanced the description of the local nucleosome geometry and the form and strength of the nucleosome–nucleosome interaction potential for Monte Carlo simulations of chromatin fibers of various types.[15,25] This framework is extended here to dissect the energetic contributions that regulate the folding of the nucleosome chain from force spectroscopy experiments. The analysis of the simulated force-extension curves revealed a complex overlay of different energetic terms. These reflect not only the nucleosome–nucleosome interaction potential but also the local nucleosome geometry, the NRL, and the strength of the interaction of the DNA with the histone octamer protein core in the context of the nucleosome.

METHODS

Chromatin Fiber Models

A coarse-grained model chromatin fiber with nucleosomes approximated by spherocylindric potentials and connected via linker DNA segments was used. The latter were represented by line charge density and contribute to the total energy in terms of elasticity, torsion and electrostatics using Debye-Hückel approximation parameterized for a salt concentration of 100 m*M* NaCl. A detailed description of this model has been reported previously.[15,25,37,38] In the simulations, two chromatin fiber conformations were investigated that differ with respect to the local geometry of their nucleosomes namely the crossed-linker two-start helix geometry (CL) and the interdigitated one-start helix geometry (ID).[25] The fiber conformations are specified in terms of two parameters [N_{stack}, N_{step}], with N_{stack} being the number of nucleosome stacks and N_{step} the step size between connected nucleosome stacks.[37,39] For the CL two-start fiber a [2,1] geometry was derived from the crystal structure of the tetranucleosome.[11] It is appropriate for a chromatin model without linker histones and low linear mass density. As a model for a chromatin fiber with increased linear mass density the interdigitated one-start helix a [6,1] geometry was selected.[12] This model represents chromatin fibers with one linker histone per nucleosome. The parameterization according to a six-angle model for the local nucleosome geometries is given in Supporting Information Table S1.

Monte Carlo Simulations

Representative equilibrium ensembles of chromatin fiber configurations were sampled using Monte Carlo (MC) simulations. The Metropolis MC algorithm and the replica exchange procedure have been described in detail elsewhere,[15,25,37,38] and simulation parameters are listed in Supporting Information Table S2 and S3. In extension of our previous work, three additional MC moves were implemented to sample changes in the fiber contour length. The first additional MC move varied the distance between the DNA entry and exit site of the nucleosome using the stretching module for nucleosomes (Supporting Information Table S2). The second move compressed or elongated the DNA segment with the stretching modulus of DNA. The third so called crank shaft move randomly selects one bead (DNA or nucleosome) of the chain and makes a rotation by a random angle around the axis defined by the connection with the n^{th} bead with n being a predefined value.[40,41] Start structures for the simulations were chosen from the ensemble of conformations in thermal equilibrium in the absence of an applied force. For a given pulling force, the MC simulations were conducted until thermal equilibrium was reached, and after computing at least 50 uncorrelated conformations. Then, the simulation was continued until another 250 uncorrelated conformations were sampled. The corresponding number of MC steps were calculated as described.[15] Depending on the conformation of the nucleosome, the pulling force, the interaction strength between DNA and histone core in the nucleosome unwrapping potential (see below) and E_{max}, 2.5×10^7 up to 2×10^8 MC steps were simulated. Simulation setups with maximal nucleosome interaction energy $E_{max} \leq 6\ k_BT$ were calculated with the Metropolis Monte Carlo algorithm. For higher nucleosome–nucleosome interaction energies a replica exchange procedure was used as introduced previously.[15] Depending on the nucleo-

some–nucleosome interaction strength 32 to 512 temperatures determined by the algorithm of Katzgraber et al.[42] were used for a given simulation. Unless otherwise noted nucleosome chains simulated had 100 nucleosomes. The stretching of the chromatin fiber was implemented by a potential including a term for the fixation of the fiber at one end and a "pulling" term applied at the other end (see Supporting Information Figure S1). The energy E_{pull} of the potential was calculated according to references 41 and 43:

$$E_{\text{pull}} = \frac{1}{2} k_{\text{hold}} \cdot v^2 - F_{\text{pull}} \cdot l_z \quad (1)$$

For an applied force F_{pull}, this potential affects the chromatin fiber equilibrium conformation in favor of an extended conformation as represented by enlarging l_z, the distance between the first and the last segment of the fiber in z-direction. Attachment of the start of the chain at the origin was implemented via the parameter k_{hold} (Supporting Information Table S2). The value of k_{hold} was chosen such that the displacement of the first segment with respect to the point of fixation would not increase more than ~0.3 nm during the simulations (see Supporting Information Text S1 for additional details).

Unwrapping of DNA from the Histone Protein Core

During extension of the nucleosome chain the nucleosomal DNA may partially unwrap from the histone protein core.[44–48] To account for this an additional homogenous unwrapping potential was included based on the analytical approach of Kulić and Schiessel.[45,49] The simplification of not accounting explicitly for the 14 distinct interaction sites of the DNA with the histone octamer core identified previously[50,51] would be relevant for a single nucleosome. However, since in our simulations chains of at least 17 nucleosomes were studied for an ensemble of conformations in thermal equilibrium individual unwrapping events occurring at a single nucleosome cannot be resolved in our simulated force-extension curves. Accordingly, the use of a simpler homogenous potential is justified. The approach is derived from analogy of a DNA spool under tension. The potential considers the pulling force, the DNA - histone core adhesion and the DNA bending deformation energy. For computing this potential the simplified form introduced in Ref. 49 was implemented:

$$E_{\text{uw,nuc}}(\vec{d}) = 2R\left(k_{\text{ad}} - \frac{A}{2R^2} - F\right) \cdot \alpha + 2FR \cdot \cos\alpha \cdot \sin\alpha + 8 \cdot \sqrt{AF} \cdot \left(1 - \sqrt{\frac{1+(\cos\ \alpha)^2}{2}}\right) + F\frac{d_z}{|\vec{d}\,|} \cdot |\Delta\vec{d}\,| \quad (2)$$

It takes advantage of the simultaneous changes of the angle α describing the amount of unwrapped DNA and the DNA pitch angle β (Supporting Information Figure S2) so that the energetically most favorable path for nucleosome unwrapping is obtained for $\alpha = \beta$ (see Supporting Information Text S1).[49] In Eq. (2), R is the radius of the nucleosome minus the radius of the DNA, k_{ad} is the interaction strength between nucleosomal DNA and the histone proteins, A is the DNA stiffness, F is the applied force, and d is the distance between the first and last contact of the DNA with the histone proteins (see Supporting Information Figure S2). For application in our model, the angle α was converted into the parameter d used in the six-angle model of the nucleosome geometry as described in the Supporting Information Text S1. The energy of the unwrapping potential was calculated according to Eq. (2) for each nucleosome after the MC moves in dependence of the parameter d in the range of $d \geq 8$ and $d \leq 50$ nm (See Supporting Information Text S1 for further details). Values of $d < 8$ nm were accounted for by the previously used potential,[15] while $d > 50$ nm corresponds to the fully unwrapped state. Accordingly, this length regime was described with the stretching potential for pure DNA. For all simulations with $k_{\text{ad}} > 2\ k_{\text{B}}T\ \text{nm}^{-1}$ the replica exchange algorithm was used to ensure that thermal equilibrium was reached.[15] In the potential given above, the adsorption energy k_{ad} in units of $k_{\text{B}}T\ \text{nm}^{-1}$ has to compensate the energy required for bending the DNA around the nucleosome and referred to here as k_{bend} with a value of $1.3\ k_{\text{B}}T\ \text{nm}^{-1}$.[45,49] Thus, the total binding energy of DNA interactions with the histone octamer core k_{bin} in the absence of an external force is calculated as $k_{\text{bin}} = k_{\text{ad}} - k_{\text{bend}}$.

RESULTS AND DISCUSSION

Force-Extension Curves of Simulated Chromatin Fibers Identify Conformational Changes of Fiber Organization

The successful application of our MC simulation framework to the simulation of DNA force spectroscopy experiments has been described recently,[43] and is also shown in Supporting Information Figure S3. This approach was extended here to studies of chromatin fibers. In Figure 1, an exemplary data set for the simulated extension of a CL fiber is presented. During the stretching simulation four different regimes can be identified: (i) At low pulling forces the chromatin fiber was straightened in the direction of the pulling force (Figure 1, regime 1). The associated energy changes were relatively small and mostly entropic (Supporting Information Figure S4). (ii) Subsequently, the slope of the force-extension curve increased because energy was needed to unstack the nucleosomes (Figure 1, regime 2). From this part approximations for the nucleosome–nucleosome interaction energy have been derived in experimental force-extension curves.[27,29] (iii) The increasing distance between nucleosomes then resulted in an apparent plateau, as nucleosome–nucleosome interactions were still significant (Figure 1, regime 3).[28,33] The nucleosome interaction energy term and the electrostatic repulsion energy from the DNA decreased upon further extension (Supporting Information Figure S4). (iv) Near the maximal extension the force increased steeply (Figure 1, regime 4). At a force of ~15 pN, the stretching and bending energy terms of the DNA and nucleosomes dominated. The simulations in Figures 1 to 4 included neither the unwrapping of DNA from the nucleosome nor the complete eviction

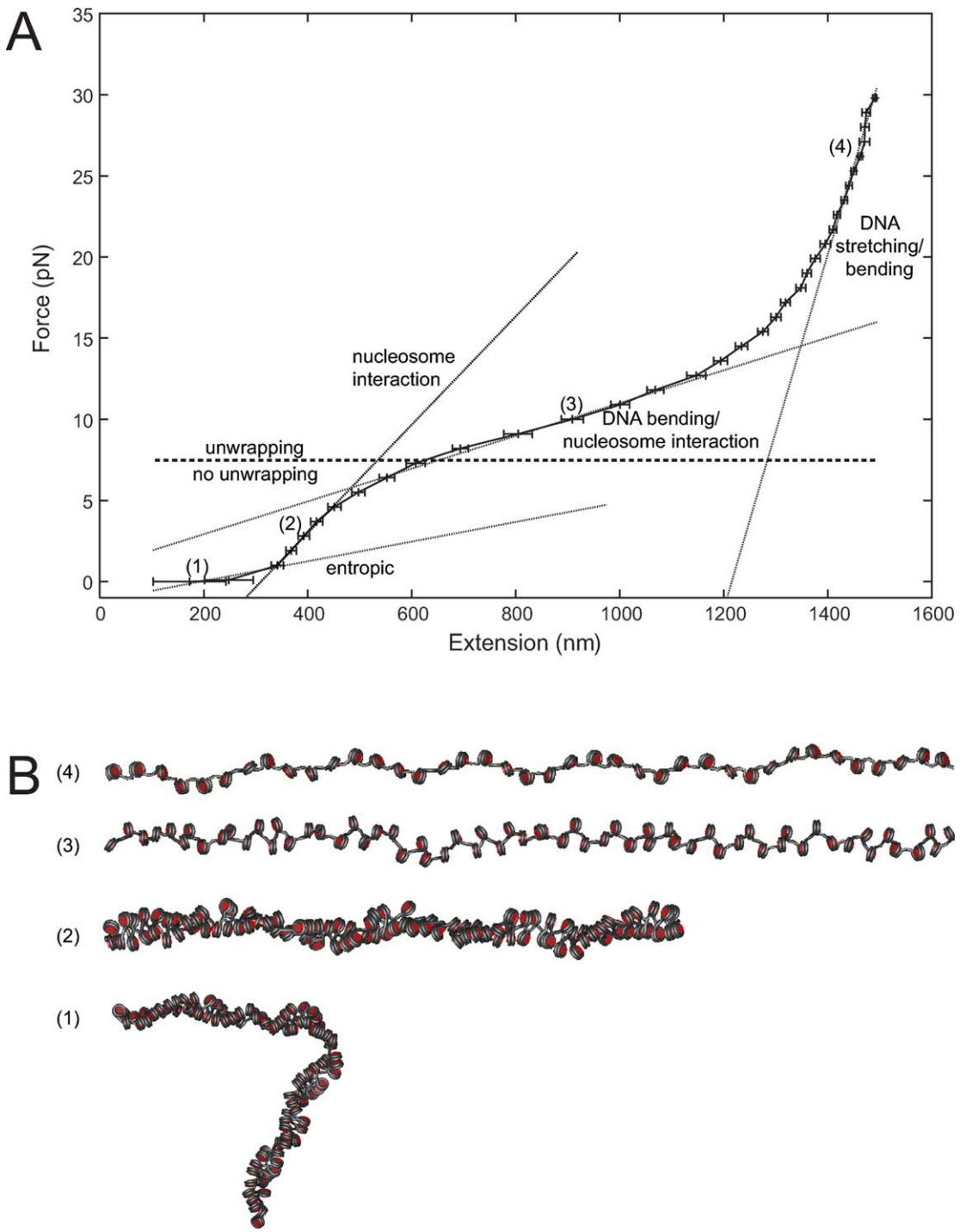

FIGURE 1 Dissection of the simulated force-extension curve of a chromatin fiber into four different regimes. A: For the example shown up to 350 nm the chromatin fiber is straightened without significant changes in its internal structure (1). From 350 to 500 nm the interactions between the nucleosomes in the fiber are weakened (2). In the range of 500 to 1200 nm the interactions between nucleosomes are broken while some DNA bending remains (3). In this regime, the unwrapping of nucleosomes would occur, which is not included in this simulations but in the comparison with the experimental data sets (Figure 5). Above 1200 nm, the dominant contributions come from straightening and stretching of the DNA (4). B: Typical configurations at pulling forces of 0.1 pN (1), 2.8 pN (2), 10 pN (3), and 28 pN (4). Numbers 1–4 correspond to the indicated sections of the force extension curve in panel A.

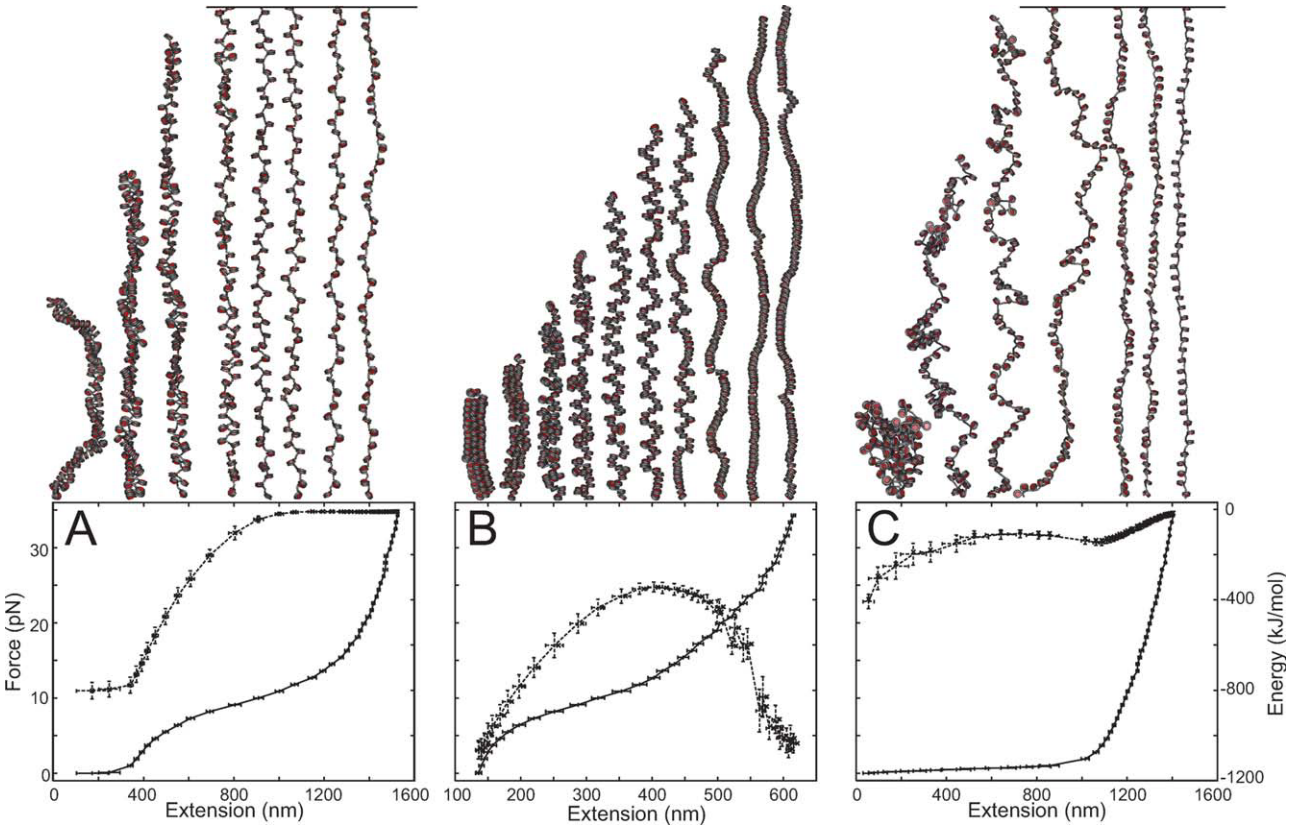

FIGURE 2 Simulated force extension curves for different fiber conformations. All simulations were performed with 6 k_BT maximal nucleosome interaction energy. For three different fibers the force-extension curve (+) is shown in comparison with the nucleosome–nucleosome interaction energy (×). A: For a fiber with CL nucleosome geometry the nucleosome–nucleosome interaction energy became insignificant in the middle of the plateau. B: Due to a reorganization of the nucleosomes in the ID geometry fiber the nucleosomal interaction energy increased again in the second half of the force-extension curve. C: Force-extension curves did not display an increased initial slope if nucleosome interactions are weak, as shown in the example for a fiber with a relatively large NRL of 207 base pairs (bp) that is associated with an increased electrostatic repulsion.

of single nucleosomes. Nevertheless, this simplified description is already sufficient to make a number of relevant conclusions.

The Contribution of Nucleosome–Nucleosome Interactions Depends on the Fiber Geometry

The interaction energy between nucleosomes strongly influenced the slope and the plateau in the first part of the force-extension curve (Figure 1, regime 2 and 3, respectively). In the MC simulations, it is instructive to make a distinction between the maximum energy value E_{max} for the optimal stacking of two nucleosomes as opposed to the effective interaction energy E_{eff} between two nucleosomes in the context of a fiber. The latter value is usually lower, since it represents the average over different orientations of two nucleosomes in a specific fiber conformation, in which optimal stacking is present only for a fraction of nucleosomes.[25] In all fibers with E_{eff} below $\sim$2 k_BT/nucleosome, the plateau was absent and the force-extension curve had a shallow slope (Figures 2C, 3C, 4C, Supporting Information Figure S5 and Table I). Increasing the effective nucleosome–nucleosome interaction energy above $\sim$2 k_BT led to a distinct separation of the entropic extension from the regime at which nucleosome–nucleosome interactions were broken (Figures 2A, 2B, 4C, and Supporting Information Figure S5). This effect was independent of the NRL and the local geometry of the nucleosome for the fibers studied here. Thus, we conclude that the presence of a distinct plateau in the initial force-extension curve is indicative of E_{eff} being $\geq$2 k_BT.

A further analysis of the mean effective nucleosome–nucleosome interaction energy reveals that it approached its

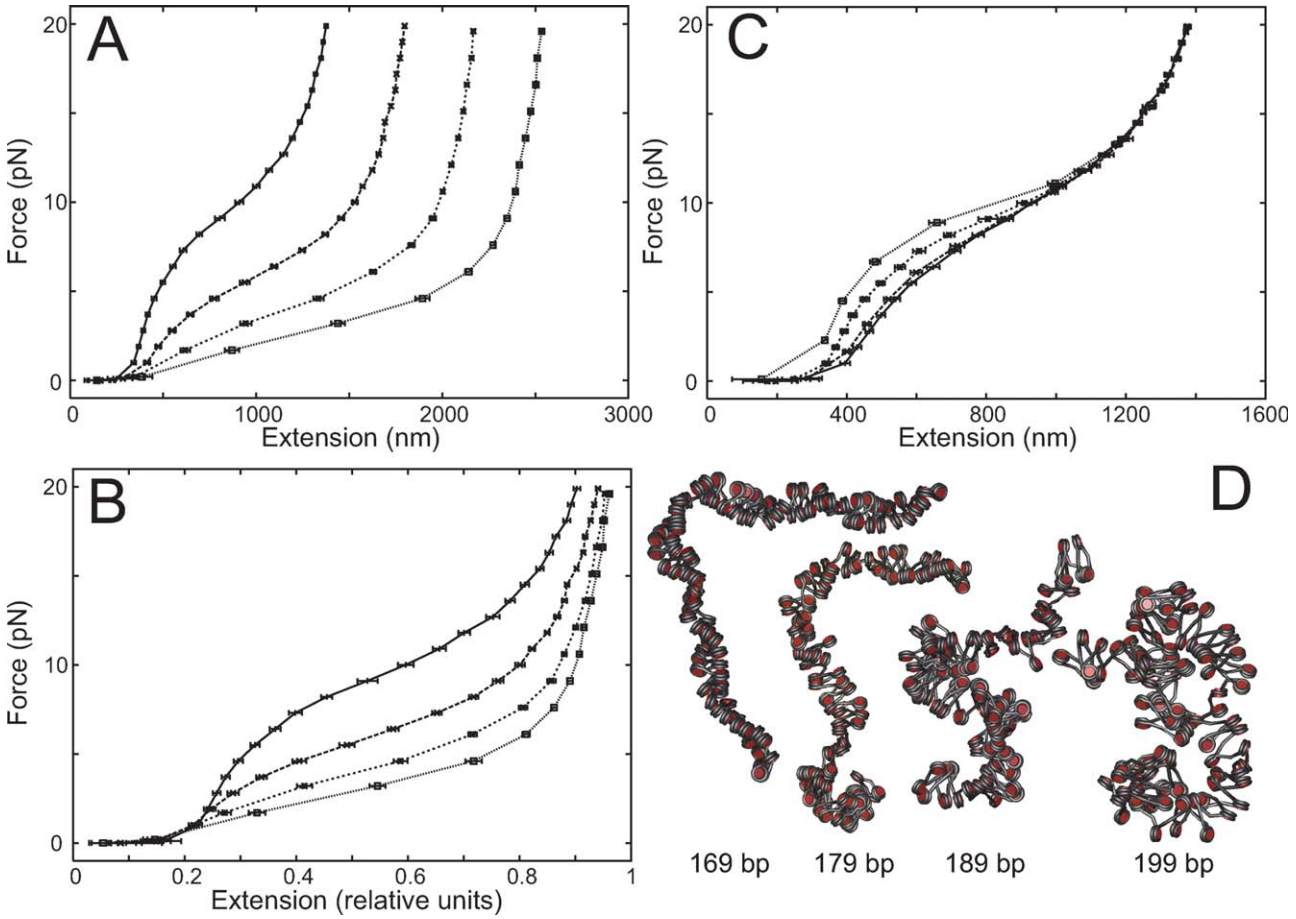

FIGURE 3 Force-extension curves for different fiber parameters of the CL nucleosome geometry. A: Extending the NRL from 169 bp (+) to 179 bp (×), 189 bp (*) and 199 bp (□) increased the total length of the stretched fiber, but the initial slope increase of the curve disappeared. B: To evaluate how the beginning of the curve is affected by the nucleosomal interaction energies the curves shown in panel A were normalized to the same length when fully extended. C: Increasing the maximal nucleosome interaction potential from 1.5 k_BT (+), 3 k_BT (×), 6 k_BT (*), to 9 k_BT (□) increased the slope at the initial part of the force-extension curve. D: Typical configurations in thermodynamic equilibrium for fibers with CL nucleosome geometry and different NRLs in the absence of an external force.

minimum around the plateau saddle point (see Figure 2). CL type fibers showed a complete loss of interaction between nucleosomes (Figure 2A). In contrast, ID geometry fibers with high effective nucleosome–nucleosome interaction energies (Figures 2B and 2C) organized their nucleosomes into a new conformation that reestablished most of the stacking interactions between them. This one-dimensionally stacked state required the local nucleosome features introduced to represent the presence of linker histone H1 in the ID fiber type.[25] For this conformation, the energy required for bending and twisting the DNA to adopt a continuous DNA wrapping around the one-dimensional nucleosome stack was lower than in the CL-geometry, and could be compensated by the favorable nucleosome–nucleosome interactions in the presence of the applied pulling force for $E_{max} = 6\ k_BT$ (Supporting Information Figure S4). At higher E_{max} values this type of reorganization also appeared to some extend with CL type fibers (data not shown). We conclude that for certain local nucleosome geometries nucleosome–nucleosome interactions can be reestablished in a new conformation after the initial destacking event. This obscures the extraction of values for the strength of the internucleosomal interactions.

High values of E_{eff} of ~10 k_BT could result in a plateau region of the force-extension curves that originated from the back folding of the fiber into hairpin structures that were stabilized by a lateral attraction of nucleosomes (data not shown).[15] Mergel et al.[36] observed a similar behavior albeit at E_{max} of 4 k_BT. As discussed previously, the use of a spherical

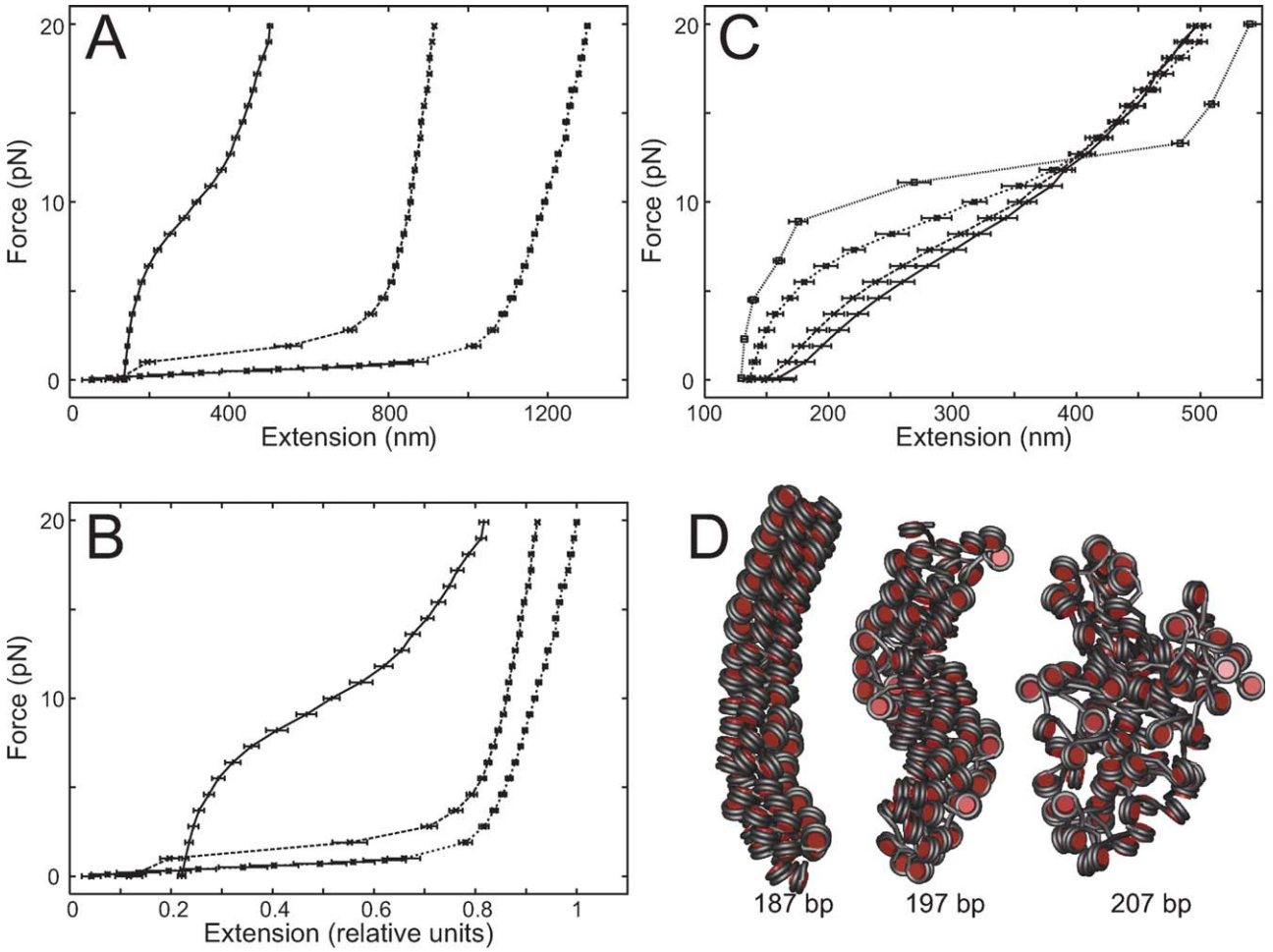

FIGURE 4 Force-extension curves for chromatin fibers with interdigitated (ID) nucleosome conformation. A: Extending the NRL from 187 bp (+) to 197 bp (×) and 207 bp (*) increased the total length of the stretched fiber, but the initial slope increase of the curve disappeared, similar to the behavior of the CL fibers in Figure 3. B: To evaluate how the beginning of the curve is affected by the nucleosomal interaction energies the curves shown in panel A were normalized to the same length when fully extended. C: Increasing the maximal nucleosome interaction potential from 1.5 k_BT (+), 3 k_BT (×), 6 k_BT (*), to 9 k_BT (□) increased the slope at the initial part of the force-extension curve. D: Typical configurations in thermodynamic equilibrium for fibers with ID nucleosome geometry and different NRLs in the absence of an external force for $E_{max} = 6\ k_BT$.

Table I Mean Effective Interaction Energies Per Nucleosome of Simulated Chromatin Fibers

	E_{eff}: CL-geometry (k_BT)				E_{eff}: ID-geometry (k_BT)		
E_{max}	169 bp	179 bp	189 bp	199 bp	187 bp	197 bp	207 bp
1.5 k_BT	0.4 ± 0.0	0.2 ± 0.0	0.1 ± 0.0	0.1 ± 0.0	0.5 ± 0.1	0.2 ± 0.0	0.1 ± 0.0
3.0 k_BT	1.1 ± 0.1	0.6 ± 0.1	0.4 ± 0.1	0.2 ± 0.0	1.4 ± 0.1	0.5 ± 0.1	0.2 ± 0.0
6.0 k_BT	3.3 ± 0.1	2.6 ± 0.2	1.9 ± 0.2	1.4 ± 0.2	4.4 ± 0.2	2.8 ± 0.2	1.6 ± 0.2
9.0 k_BT	7.3 ± 0.2	5.7 ± 0.2	5.3 ± 0.2	4.7 ± 0.2	7.8 ± 0.2	6.8 ± 0.2	4.3 ± 0.2

E_{max} and E_{eff} are the maximal and effective nucleosome interaction energy per nucleosome in the MC simulation. See text for further description of these parameters.

or ellipsoidal nucleosome–nucleosome interaction potential stabilizes the back-folded conformation at lower energies as compared to the spherocylindric potential used here.[15] It is also noted that both experimental and modeling studies indicate that histone tails are important for mediating internucleosomal interactions.[24,52,53] Furthermore, in the cell the higher order folding of the nucleosome chain could be enhanced by architectural chromosomal proteins.[54,55] Back folding can be neglected for short fibers like those with 17 and 25 nucleosomes that are compared below with experimental measurements.

Previously, the interaction energy between nucleosomes has been calculated by integrating a certain area of experimentally determined force-extension curves, which corresponds to regime 2 or 3 in Figure 1.[27,28] From dissecting the relative contributions of all energetic contributions in our MC simulations, it becomes apparent that all energy terms are significant in these two regimes (Supporting Information Figure S4). The nucleosome–nucleosome interaction energy is responsible for the presence or absence of the initial increase and/or the subsequent plateau of the force extension curve. However, the slope of the initial increase and the plateau height are controlled by a combination of different energetic and conformational parameters. Thus, no simple relation exists to extract the interaction energy between nucleosomes from the force-extension curves. However, by using E_{max} as a fitting parameter in the simulations of a certain fiber conformation the nucleosome–nucleosome interaction energy can be retrieved as described in the following.

Different Parameter Combinations of Nucleosome Geometry, Repeat Length, and Interaction Potential can Result in Similarly Shaped Force-Extension Curves

The contribution of the nucleosome repeat length was investigated as an additional parameter that determines the chromatin fiber conformation (Figures 3A and 4A). At increasing NRL the slope in the transition between regime 1 and 2 was reduced due to an increased electrostatic repulsion of the DNA. The latter enlarged the distance between adjacent nucleosomes, and thus lowered the effective nucleosome–nucleosome interaction energies E_{eff} (Table I). This effect was independent of the local nucleosome geometries and/or the specific value of E_{max}. To account for differences in the contour length due to variations of the NRL and to better visualize differences, the force-extension curves in Figures 3B and 4B were normalized to the same length at a pulling force of 35 pN. At this point the simulated chain is almost completely extended and the energy needed for further stretching is mostly due to DNA stretching and bending.

In addition to variations in the electrostatics due to the presence or absence of linker histones, changes in the local geometries of nucleosomes can favor reorganizations of the nucleosomes in fibers with applied stretching forces. The force-extension curve of the interdigitated fiber with an NRL of 187 bp and E_{max} of 9 k_BT (Figure 4C) was shifted to higher extensions compared to curves with lower E_{max} at pulling forces above 13 pN due to the reorganization of nucleosome stacks.

By varying parameters like the nucleosome interaction energy E_{max} and the nucleosome repeat length a similar-shaped normalized force-extension curve can be found for both the CL and ID geometry (Supporting Information Figure S5). Thus, it is not straightforward to distinguish between chromatin fiber conformations solely from the shape of the force-extension curve (Supporting Information Figure S5) (Table I). Nevertheless, for the same chain conformation with respect to the local nucleosome geometry and the NRL, the normalized curves can be used to identify differences in the effective nucleosome–nucleosome interaction energy from the initial slope and plateau of the curves.

Comparison of Simulated and Experimental Force-Extension Curves Allows The Evaluation of Nucleosome–Nucleosome Interaction Energies

We analyzed an experimental force-extension curve without linker histones from a previous study with arrays of the 601 nucleosome-positioning DNA with 25 nucleosomes and a NRL of 197 bp.[29] For the simulations, we used the same number of nucleosomes and repeat length flanked by ~150 bp linker DNA at both ends to mimic the experimental system described in Ref. 29. A CL-geometry was chosen since the shape of this type of model fiber was in good agreement with electron microscopic images of experimentally used fibers (see Figure 4 of Ref. 16). Simulated force-extension curves of E_{max} 16 and 18 k_BT behaved similar to the experimental measurement (Figure 5A). These values result in effective internucleosomal energies of 12.7 to 14.8 k_BT. This confirms the high nucleosome interaction energy of 14 k_BT derived previously from the experiments.[29]

While the experimental curve starts between 0 and 100 nm all simulated force-extension curves were shifted by about 50 nm and display a contour length of 120 ± 25 nm at zero force. It is noted that the 293 bp of flanking DNA in the nucleosome chain alone amount to 100 nm. A contour length of 150 nm is expected for the folded fiber and 770 nm for the fully extended chain as calculated in Ref. 29. Thus,

there appears to be an offset present for the experimental data sets. For the simulations, the nucleosome unwrapping potential was included that is described in Materials and Methods. Below 300 nm extension or 4 pN force its contribution is negligible. Above this value the nucleosome unwrapping is reflected in the formation of a plateau (Figure 5A). However, as the experimental data are restricted to the low force regime below 5.5 pN only little information on the strength of the interaction between the DNA and the histone octamer core can be retrieved from this data set. Furthermore, the height of the plateau mostly reflects the strength of the internucleosomal interaction as apparent from comparing the different simulated curves.

To evaluate the behavior of a chromatin fiber over a larger force range up to 20 pN a second set of comparisons with the experimentally measured force-extension measurements from Brower-Toland et al.[30] was conducted. In these a fiber with 17 nucleosomes and an NRL of 208 bp and 150 bp flanking DNA at both fiber ends was studied (Figures 5B and 5C). Since the experiments were conducted without linker histones the CL-nucleosome geometry was chosen for these simulations, too. For the evaluation of the nucleosome–nucleosome interactions the low force regime up to about 5 pN is most relevant. Up to a corresponding extension of ~450 nm the simulated force-extension curve fits well if a value of $E_{max} \leq 9\ k_BT$ was used for the maximum strength of the nucleosome interaction potential (Figure 5B, light blue curve). For $E_{max} \geq 12\ k_BT$ the simulated force-extension curves displayed an initial slope that was not present in the experiments (Supporting Information Figure S6). An evaluation of the different energy terms in our simulations revealed that the electrostatic repulsions of the ~60 bp long linker DNA prohibits establishing strong nucleosome–nucleosome interactions so that the energetic contribution from this term to the total fiber energy was relatively small, yielding $E_{eff} = 2.3 \pm 0.7\ k_BT$. This is similar to the value of 3.4 k_BT reported previously for fibers isolated from chicken erythrocytes.[28]

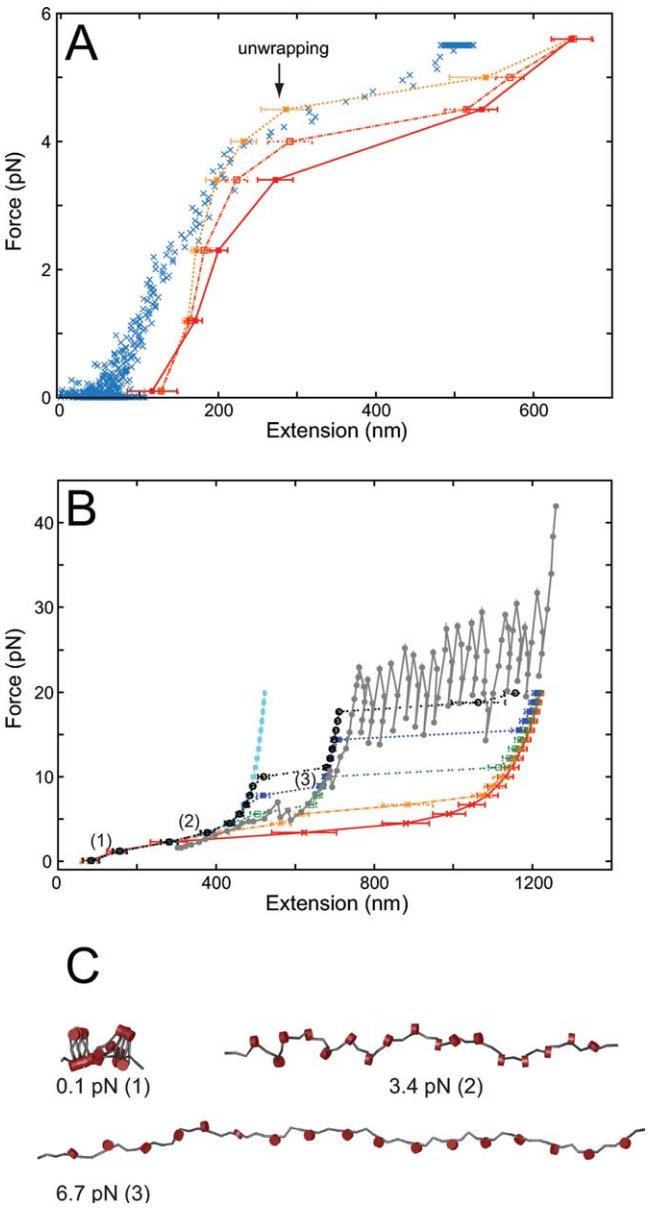

FIGURE 5 Comparison of simulations and experimental force-extension curves. A: Comparison of a experimentally measured force-extension curve of a 25 nucleosome chromatin fiber without linker histones[29] with curves of simulated chromatin fibers. For the experimental curve measurements are shown by the blue crosses. The simulated curves were calculated with an unwrapping parameter $k_{ad} = 4\ k_BT\ nm^{-1}$ and a maximal nucleosome interaction energy E_{max} of 14 k_BT (red), 16 k_BT (dark orange) and 18 k_BT (light orange). The arrow marks the beginning of DNA unwrapping from the histone core in the simulation. (B) Experimental force spectroscopy curve for a chain of 17 nucleosomes in the absence of linker histones (gray)[30] in comparison with corresponding simulated force-extension curves. All fibers were simulated with a maximal nucleosome interaction energy of 9 k_BT. The simulated fiber is in good agreement with the experimental curve for the first 500 nm in the absence of DNA unwrapping (light blue). If the DNA unwrapping potential was included in the simulations the fit with the experimental data was largely improved. Simulations are shown for different interaction strength between DNA and histones with values for k_{ad} of 2 (red), 3 (orange), 4 (green), 5 (dark blue), and 6 $k_BT\ nm^{-1}$ (black). See text for further details. C: Typical configurations in thermodynamic equilibrium of the chain with 17 nucleosomes in CL type fiber conformation at different applied pulling forces and including the nucleosome unwrapping potential with $k_{ad} = 4\ k_BT\ nm^{-1}$. The numbers correspond to the regions of the force-extension curve indicated in panel B. The nucleosomes are visualized as red cylinders. The gray DNA in between the nucleosomes contains the linker and the unwrapped DNA.

This observation is in good agreement with our previous MC studies of fibers with the CL nucleosome geometry, in which open structures with very low fiber mass density were present for an NRL of 199 bp[25] (Figure 5C, 0.1 pN). In addition, electron microscopy images of fibers without linker histones show very similar structures with strongly reduced contacts between nucleosomes for NRLs above 190 bp.[16] In the first 500 nm of extension all simulated curves were ~30 nm shorter than the experimental values. As discussed above this may reflect an offset of the experimental data.

The effective nucleosome–nucleosome interaction energy derived from the force-extension curve of Brower-Toland et al.[30] (Figure 5B) is ~6 times lower than the values from the curve determined by Kruithof et al.[29] (Figure 5A). This difference can be rationalized in terms of two differences between the chromatin fibers studied. The NRL of the fiber studied in Ref. 30 is 10 bp larger. This opposes nucleosome–nucleosome interactions due to higher electrostatic repulsion of the DNA[25] and would lead to a lower value of E_{eff}. In addition, different nucleosome positioning sequences were used, namely the strong 601 DNA positioning sequence[29] and the sea urchin 5S nucleosome positioning element.[30] The 5S rDNA sequence has one major and several secondary nucleosome binding sites,[56] which may introduce some variations in nucleosome spacing. This is not accounted for in our simulations. In contrast, the fibers from the Kruithof et al. study have been shown to have a exceptionally high regular nucleosome occupancy.[57] As demonstrated previously any variation of nuclear spacing is expected to weaken the effective internucleosomal interactions within the fiber.[25] The above-mentioned differences in the conformation of the nucleosome chain could explain the variations in the effective internucleosomal interaction energy between the two studies to some extend. However, it is noted that also the intrinsic strength of the nucleosome–nucleosome interactions for the optimal stacking of two nucleosomes derived from our simulations, i.e., the parameter E_{max}, was quite different namely about ~16 $k_{\mathrm{B}}T$ (Fig. 5A) versus 9 $k_{\mathrm{B}}T$ (Fig. 5B). This points to differences in the fiber composition and/or the solvent environment that are not considered in our analysis as for example the presence of 0.02% (vol/vol) Tween 20 detergent in Ref. 30. Furthermore, in a recent theoretical study,[53] it was concluded that acetylation of a single histone H4 tail at lysine 16 can reduce the internucleosomal interaction energy by almost 2 $k_{\mathrm{B}}T$. This is in line with experimental observations demonstrating a striking unfolding of nucleosomal arrays and chromatin fibers upon H4K16 acetylation.[23,24] Since the experiments discussed here in the context of Figure 5 were conducted with purified native histone octamers, it is conceivable that variations in the degree of histone acetylation between different fiber preparations contribute to the results. As demonstrated previously, the effect of in vitro acetylation of histones H3 and H4 is clearly apparent in the force spectroscopy curves, albeit mostly with respect to weakening histone-DNA interactions.[31]

DNA Unwrapping Starts at Forces Above ~4 to 5 pN and the Outer DNA Turn is Bound Less Stably to the Histone Octamer Core Than the Inner DNA Turn

To account for the process of DNA unwrapping in the MC simulations an analytically derived potential was implemented in our coarse-grained model as described in the Methods section.[45,49] For an isolated nucleosome experimental studies indicate that DNA unwrapping starts already at forces as low as ~3 pN.[46,47] In contrast, for the chain of 25 nucleosomes analyzed in Figure 5A no unwrapping of nucleosomes below pulling forces of 6–7 pN has been reported.[27,29] This has been deduced from the lack of a hysteresis in the plateau starting at ~200 nm extension. In the simulations conducted here for this system with $E_{\mathrm{max}} = 18$ $k_{\mathrm{B}}T$ no significant unwrapping was present in the trajectories up to forces of 4.5 pN. Above this value at the beginning of the plateau, nucleosome unwrapping became significant in the simulations. Reducing the value of E_{max} led to a decrease of the force at which unwrapping starts (Figure 5A). Thus, the interactions between nucleosomes within the chromatin fiber stabilized the nucleosome structure and counteracted DNA unwrapping. This conclusion is also supported by experimental studies of the disruption of the nucleosome via histone binding to the histone chaperone NAP1. It was found that an H2A · H2B dimer could be extracted from mononucleosomes but not from a nucleosome chain folded into a fiber.[58,59]

For the second data set analyzed in our simulations unwrapping was clearly required to account for the shape of the experimental force-extension curve above 4–5 pN (Figure 5B). A comparison over the complete extension range shows that unwrapping with a constant value for the adsorption energy k_{ad} was not appropriate for an accurate description of the complete unwrapping process. This behavior can be rationalized in terms of the nucleosome structure.[60,61] The outer turn (67 bp, 23 nm of DNA) is unwrapped first and more easily than the inner DNA turn (80 bp, 27 nm) as proposed previously.[30,31,44–46,48,62] For the data set analyzed in Figure 5B, an adsorption strength of 2–3 $k_{\mathrm{B}}T\,\mathrm{nm}^{-1}$ yielded a good agreement with the first part of the DNA-histone dissociation process. For the energetics of this process values of 10 $k_{\mathrm{B}}T$,[46] 15 $k_{\mathrm{B}}T$,[63] and 20 $k_{\mathrm{B}}T$[30] have been derived from force spectroscopy as well as competitive protein binding

experiments. The potential and parameter used here (k_{ad} = 2.5 k_BT nm^{-1}, k_{bend} = 1.3 k_BT nm^{-1}) correspond to energetic costs of k_{bin} = 1.2 k_BT nm^{-1} or 28 k_BT in total for breaking DNA-histone interactions in this part of the nucleosome.

For further unwrapping, i.e., extensions larger than 700 nm, an energy barrier exists (Figure 5B).[30,44,64] In the unwrapping potential, the barrier reflects the energy needed to bend the linker DNA, which is required to unwrap the second turn of the nucleosome in the direction of the applied force.[45,49] In addition, it appears that higher affinity DNA histone interactions flanking the dyad axis contribute to this behavior, which is not accounted for in the simulations.[44] Korolev et al. explained the unwinding of the second turn as a result of a much larger change in the electrostatic free energy than the first turn.[64] From the comparison of the curves, we conclude that a localized increase of the value of k_{ad} to 4–5 k_BT nm^{-1} is necessary to describe the experimental data in this regime (Figure 5B).

The saw-tooth shape structure in the force-extension curves reflects a successive and irreversible dissociation of nucleosomes from a single chromatin fiber.[30,46,65,66] This behavior is lacking in the MC simulations. Per definition, our values in the force-extension curves reflect a mean value in the equilibrium of a representative chromatin fiber ensemble at a given applied force as opposed to the time-dependent behavior of a single molecule, in which successive irreversible unwrapping events of individual nucleosomes can be resolved. While the individual unwrapping events become averaged out in the ensemble analysis they are visible in the inspection of the single MC trajectories as discrete reversible jumps in the length of the DNA associated with a single nucleosome (Supporting Information Figure S7).

CONCLUSIONS

The various types of force spectroscopy experiments of single chromatin fibers provide a wealth of information with respect to the molecular interactions and energetic terms of the nucleosome chain.[67] In addition, important conclusions on the fiber conformation and their characteristic features as for example their mass density can be made. The recent advancements in the reconstitution of chromatin fibers allow it to obtain well defined chains for the force spectroscopy experiments with respect to the nucleosome repeat length, the number of nucleosomes and linker histone stoichiometry as well as the post-translational modification state of the histones.[27,29–31,44] Here, we have focused on the comparison of our simulations with results of two of these studies, in which the NRL and the number of nucleosomes were known and linker histones were absent. While a number of models have been proposed for the folding of the nucleosome chain in the presence of linker histones the corresponding conformation is still under discussion (see for example[25,37,39,57,68] and references therein). In contrast, the crystal structure of a tetranucleosome[11] provides a better defined starting point for chromatin fiber models for nucleosome chains without linker histones in the presence of monovalent ions. The resulting fiber models as used here for the comparative analysis with experimental data are in good agreement with electron microscopy measurements.[25] One additional parameter to be considered is the effect of divalent ions of Mg^{2+} that could facilitate bending of the linker DNA. This was shown recently by Grigoryev et al. in an approach that combined electron microscopy analysis with coarse grained modeling and a phenomenological description for the increase in DNA flexibility observed in the presence of Mg^{2+}.[68] This effect is not accounted for in our current description of the DNA electrostatics, which refers to 100 m*M* NaCl. Thus, it could be a potential source of deviations when comparing the simulations to the two experimental force-extension curves depicted in Figure 5 that were acquired in the presence of 2 m*M* magnesium acetate and 100 m*M* potassium acetate[29] or 100 m*M* NaCl and 0.5 m*M* unchelated magnesium chloride.[30]

Several theoretical approaches were developed to investigate nucleosome and chromatin dynamics under tension. They can be divided in two major groups. The first group focuses on a single nucleosome and provided considerable insight into the interactions between DNA and histone core.[45,46,62] As shown here for the implementation of a previously derived unwrapping potential the resulting quantitative descriptions can be subsequently integrated into coarse-grained descriptions to model the behavior of chromatin fibers in response to an external force via MC simulations to reveal chromatin fiber features. A previous study applied MC simulations to the low force regime of force-extension curves to derive the persistence lengths and elastic moduli of a chromatin fiber.[35] Our study extends this work by using a further developed fiber model. It focuses on the implementation of an approach that dissects specific energy terms from force spectroscopy curves over a broad range of stretching forces. The results demonstrate that this goal can be reached if some a priori knowledge of the local nucleosome geometry is available. In particular, it is apparent that nucleosome–nucleosome interaction energies estimated from the analysis of the initial part of experimental force-extension curves may be obscured by significant contributions from DNA bending and torsion, which in turn are highly dependent on the fiber conformation. Furthermore, both our simulations (see

Figure 5) as well as previous experimental studies support the view that the contribution from DNA unwrapping in the force spectroscopy experiments is also dependent on the fiber conformation.[27,29,46,47] Strong nucleosome–nucleosome interactions stabilize the fully wrapped structure so that unwrapping may become significant at different forces ranging from ~3 to 6 pN. By conducting virtual force spectroscopy experiments parameters for nucleosome–nucleosome and histone-DNA interactions were identified that yield a good agreement with the experimental data. It is anticipated that this approach will prove to be highly valuable for dissecting the local nucleosome geometry as well as the nucleosome–nucleosome and histone-DNA interaction energies from further investigations of the force-dependent chromatin fiber conformation.

The authors are grateful to Robert Schöpflin, Vladimir Teif, Gerrit Heuvelman, and John van Noort for discussions and Sofie Hofer for help with editing the manuscript. The project mvb00007 at the North German Supercomputing Alliance (HLRN) is a grant and thus needs to be removed from here to the first page.

REFERENCES

1. Henikoff, S. Nat Rev Genet 2008, 9, 15–26.
2. Robinson, P. J.; Rhodes, D. Curr Opin Genet Dev 2006, 16, 336–343.
3. Tremethick, D. J. Cell 2007, 128, 651–654.
4. Wachsmuth, M.; Caudron-Herger, M.; Rippe, K. Biochim Biophys Acta 2008, 1783, 2061–2079.
5. Poirier, M. G.; Bussiek, M.; Langowski, J.; Widom, J. J Mol Biol 2008, 379, 772–786.
6. van Holde, K. E. Chromatin; Springer: Heidelberg, 1989.
7. Luger, K. Chromosome Res 2006, 14, 5–16.
8. Hansen, J. C. Annu Rev Biophys Biomol Struct 2002, 31, 361–392.
9. Woodcock, C. L.; Skoultchi, A. I.; Fan, Y. Chromosome Res 2006, 14, 17–25.
10. Bassett, A.; Cooper, S.; Wu, C.; Travers, A. Curr Opin Genet Dev 2009, 19, 159–165.
11. Schalch, T.; Duda, S.; Sargent, D. F.; Richmond, T. J. Nature 2005, 436, 138–141.
12. Daban, J. R.; Bermudez, A. Biochemistry 1998, 37, 4299–4304.
13. Bednar, J.; Horowitz, R. A.; Grigoryev, S. A.; Carruthers, L. M.; Hansen, J. C.; Koster, A. J.; Woodcock, C. L. Proc Natl Acad Sci USA 1998, 95, 14173–14178.
14. Hamiche, A.; Schultz, P.; Ramakrishnan, V.; Oudet, P.; Prunell, A. J Mol Biol 1996, 257, 30–42.
15. Stehr, R.; Kepper, N.; Rippe, K.; Wedemann, G. Biophys J 2008, 95, 3677–3691.
16. Routh, A.; Sandin, S.; Rhodes, D. Proc Natl Acad Sci USA 2008, 105, 8872–8877.
17. Perisic, O.; Collepardo-Guevara, R.; Schlick, T. J Mol Biol 2010, 403, 777–802.
18. Gerchman, S. E.; Ramakrishnan, V. Proc Natl Acad Sci USA 1987, 84, 7802–7806.
19. Ghirlando, R.; Felsenfeld, G. J Mol Biol 2008, 376, 1417–1425.
20. Hansen, J. C.; Ausio, J.; Stanik, V. H.; van Holde, K. E. Biochemistry 1989, 28, 9129–9136.
21. van Holde, K.; Zlatanova, J. Proc Natl Acad Sci USA 1996, 93, 10548–10555.
22. Bednar, J.; Horowitz, R. A.; Dubochet, J.; Woodcock, C. L. J Cell Biol 1995, 131, 1365–1376.
23. Shogren-Knaak, M.; Ishii, H.; Sun, J. M.; Pazin, M. J.; Davie, J. R.; Peterson, C. L. Science 2006, 311, 844–847.
24. Robinson, P. J. J.; An, W.; Routh, A.; Martino, F.; Chapman, L.; Roeder, R. G.; Rhodes, D. J Mol Biol 2008, 381, 816–825.
25. Kepper, N.; Foethke, D.; Stehr, R.; Wedemann, G.; Rippe, K. Biophys J 2008, 95, 3692–3705.
26. Sun, J.; Zhang, Q.; Schlick, T. Proc Natl Acad Sci USA 2005, 102, 8180–8185.
27. Kruithof, M.; Chien, F.; de Jager, M.; van Noort, J. Biophys J 2008, 94, 2343–2348.
28. Cui, Y.; Bustamante, C. Proc Natl Acad Sci USA 2000, 97, 127–132.
29. Kruithof, M.; Chien, F.-T.; Routh, A.; Logie, C.; Rhodes, D.; van Noort, J. Nat Struct Mol Biol 2009, 16, 534–540.
30. Brower-Toland, B. D.; Smith, C. L.; Yeh, R. C.; Lis, J. T.; Peterson, C. L.; Wang, M. D. Proc Natl Acad Sci USA 2002, 99, 1960–1965.
31. Brower-Toland, B.; Wacker, D. A.; Fulbright, R. M.; Lis, J. T.; Kraus, W. L.; Wang, M. D. J Mol Biol 2005, 346, 135–146.
32. Bancaud, A.; Conde e Silva, N.; Barbi, M.; Wagner, G.; Allemand, J.-F.; Mozziconacci, J.; Lavelle, C.; Croquette, V.; Victor, J.-M.; Prunell, A.; Viovy, J.-L. Nat Struct Mol Biol 2006, 13, 444–450.
33. Schiessel, H.; Gelbart, W. M.; Bruinsma, R. Biophys J 2001, 80, 1940–1956.
34. Katritch, V.; Bustamante, C.; Olson, W. K. J Mol Biol 2000, 295, 29–40.
35. Aumann, F.; Lankas, F.; Caudron, M.; Langowski, J. Phys Rev E 2006, 73, 041927.
36. Mergell, B.; Everaers, R.; Schiessel, H. Phys Rev E 2004, 70, 011915.
37. Stehr, R.; Schöpflin, R.; Ettig, R.; Kepper, N.; Rippe, K.; Wedemann, G. Biophys J 2010, 98, 1028–1037.
38. Wedemann, G.; Langowski, J. Biophys J 2002, 82, 2847–2859.
39. Depken, M.; Schiessel, H. Biophys J 2009, 96, 777–784.
40. Binder, K. In Computer Simulation of Polymers; Colbourn, E. A., Ed.; Longman Scientific and Technical: Harlow, 1994; pp 91–129.
41. Vologodskii, A. V.; Marko, J. F. Biophys J 1997, 73, 123–132.
42. Katzgraber, H. G.; Trebst, S.; Huse, D. A.; Troyer, M. J Stat Mech 2006, 2006, P03018.
43. Maffeo, C.; Schöpflin, R.; Brutzer, H.; Stehr, R.; Aksimentiev, A.; Wedemann, G.; Seidel, R. Phys Rev Lett 2010, 105, 158101–158101.
44. Hall, M. A.; Shundrovsky, A.; Bai, L.; Fulbright, R. M.; Lis, J. T.; Wang, M. D. Nat Struct Mol Biol 2009, 16, 124–129.
45. Kulić, I. M.; Schiessel, H. Phys Rev Lett 2004, 92, 228101.
46. Mihardja, S.; Spakowitz, A. J.; Zhang, Y.; Bustamante, C. Proc Natl Acad Sci USA 2006, 103, 15871–15876.
47. Kruithof, M.; van Noort, J. Biophys J 2009, 96, 3708–3715.
48. Teif, V. B.; Ettig, R.; Rippe, K. Biophys J 2010, 99, 2597–2607.

49. Kulic, I. M.; Schiessel, H. In DNA Interactions with Polymers and Surfactants; Dias, R. S.; Lindman, B., Eds.; Wiley: London, 2008; pp 173–208.
50. Luger, K.; Mäder, A. W.; Richmond, R. K.; Sargent, D. F.; Richmond, T. J. Nature 1997, 389, 251–260.
51. Luger, K.; Richmond, T. J. Curr Opin Struct Biol 1998, 8, 33–40.
52. Arya, G.; Schlick, T. Proc Natl Acad Sci USA 2006, 103, 16236–16241.
53. Yang, D.; Arya, G. Phys Chem Chem Phys 2011, 13, 2911–2921.
54. Woodcock, C. L. Curr Opin Genet Dev 2006, 16, 213–220.
55. McBryant, S.; Adams, V.; Hansen, J. Chromosome Res 2006, 14, 39–51.
56. Dong, F.; Hansen, J. C.; van Holde, K. E. Proc Natl Acad Sci USA 1990, 87, 5724–5728.
57. Robinson, P. J.; Fairall, L.; Huynh, V. A.; Rhodes, D. Proc Natl Acad Sci USA 2006, 103, 6506–6511.
58. Kepert, J. F.; Mazurkiewicz, J.; Heuvelman, G.; Fejes Tóth, K.; Rippe, K. J Biol Chem 2005, 280, 34063–34072.
59. Mazurkiewicz, J.; Kepert, J. F.; Rippe, K. J Biol Chem 2006, 281, 16462–16472.
60. Battistini, F.; Hunter, C. A.; Gardiner, E. J.; Packer, M. J. J Mol Biol 2010, 396, 264–279.
61. Richmond, T. J.; Davey, C. A. Nature 2003, 423, 145–150.
62. Wocjan, T.; Klenin, K.; Langowski, J. J Phys Chem B 2009, 113, 2639–2646.
63. Anderson, J. D.; Widom, J. J Mol Biol 2000, 296, 979–987.
64. Korolev, N.; Vorontsova, O. V.; Nordenskiöld, L. Prog Biophys Mol Biol 2007, 95, 23–49.
65. Pope, L. H.; Bennink, M. L.; van Leijenhorst-Groener, K. A.; Nikova, D.; Greve, J.; Marko, J. F. Biophys J 2005, 88, 3572–3583.
66. Ranjith, P.; Yan, J.; Marko, J. F. Proc Natl Acad Sci USA 2007, 104, 13649–13654.
67. Lavelle, C.; Victor, J.-M.; Zlatanova, J. Int J Mol Sci 2010, 11, 1557–1579.
68. Grigoryev, S. A.; Arya, G.; Correll, S.; Woodcock, C. L.; Schlick, T. Proc Natl Acad Sci USA 2009, 106, 13317–13322.

Reviewing Editor: J. Andrew McCammon

Supporting Material

Force spectroscopy of chromatin fibers: extracting energetics and structural information from Monte Carlo simulations

Nick Kepper[1], Ramona Ettig[1], Rene Stehr[2], Sven Marnach[3],

Gero Wedemann[2] and Karsten Rippe[1*]

[1] Deutsches Krebsforschungszentrum & BioQuant, Research Group Genome Organization & Function, Im Neuenheimer Feld 280, 69120 Heidelberg, Germany

[2] University of Applied Sciences Stralsund, CC Bioinformatics, Zur Schwedenschanze 15, 18435 Stralsund, Germany

[3] Interdisciplinary Center for Scientific Computing, Im Neuenheimer Feld 368, 69120 Heidelberg, Germany

* address correspondence to Karsten Rippe, Deutsches Krebsforschungszentrum, Research Group Genome Organization & Function (B066), Im Neuenheimer Feld 280, 69120 Heidelberg, Germany. Tel.: +49-6221-5451376; Fax: +49-6221-5451487;

E-mail: Karsten.Rippe@dkfz.de

Supporting Table S1. Parameters of CL- and ID-nucleosome geometries in the six-angle-model.

Fiber type	**NRL** (bp)	α (°)	β (°)	γ (°)	δ (°)	ε (°)	ϕ (°)	c (nm)	d (nm)	**diameter** (nm)	**mass density** (nuc./11 nm)
CL	169	50	140	-50	20	0	0	3.3	8	26.2 ± 0.2	3.1 ± 0.1
CL	179	35	140	-35	20	0	0	3.3	8	28.2 ± 0.3	2.8 ± 0.1
CL	189	27	140	-27	20	0	0	3.3	8	30.1 ± 0.3	2.4 ± 0.1
CL	199	22	140	-22	20	0	0	3.3	8	31.6 ± 0.3	2.2 ± 0.1
CL	208	20	140	-20	20	0	0	3.3	8	—	—
ID	187	117.5	0	-65	60	0	0	5.6	3.7	30.1 ± 0.1	7.6 ± 0.2
ID	197	117.5	0	-39	58	0	0	5.6	3.7	37.5 ± 0.4	6.9 ± 0.5
ID	207	117.5	0	-28	52	0	0	5.6	3.7	—	—

Supporting Table S2. Simulation parameters

Parameter	Value
Stretching module (DNA)	$1.10 \cdot 10^{-18}$ J nm
Bending module (DNA)	$2.06 \cdot 10^{-19}$ J nm
Torsion module (DNA)	$2.67 \cdot 10^{-19}$ J nm
Electrostatic radius (DNA)	1.2 nm
Stretching module (nucleosome)	$1.10 \cdot 10^{-18}$ J nm
Torsion module (nucleosome)	$1.30 \cdot 10^{-18}$ J nm
Fiber-ground adhesion module	$1.10 \cdot 10^{-18}$ J nm^{-2}
Temperature	293 K
Ionic strength	100 mM NaCl
S-function parameters (cylinder)	S000 = 1.6957 Scc2 = -0.7641 S220 = -0.1480 S222 = -0.2582 S224 = 0.5112 E000 = 2.7206 Ecc2 = 6.0995 E220 = 3.3826 E222 = 7.1036 E224 = 3.2870 nm

A detailed description of the S-function parameters can be found in Stehr et al.[1] Values for the stretching, bending, and torsion modules are taken from [2].

Supporting Table S3. Monte-Carlo moves

100 nucleosome fiber	17 and 25 nucleosome fiber	λ-DNA
pivot move	pivot move	pivot move
DNA stretching	DNA stretching	DNA stretching
nucleosome entry points movement	nucleosome entry points movement	bead rotation
bead rotation	bead rotation	crank shaft (5 beads loops)
crank shaft (5 beads loops)	crank shaft (5 beads loops)	crank shaft (25 beads loops)
crank shaft (25 beads loops)	crank shaft (25 beads loops)	crank shaft (100 beads loops)
crank shaft (100 beads loops)	crank shaft (50 beads loops)	crank shaft (300 beads loops)

The stretching and crank shaft moves are described in the Materials and Methods section. A detailed description of the bead rotation and pivot moves can be found in [2].

Supporting Table S4. Parameters of the unwrapping potential

Parameter	Description
A	bending stiffness of the DNA
E_{bend}	bending energy
E_{comp}	competition of adsorption and applied forces
E_{geom}	"geometrical" energy
E_{stiff}	stiffness of the non-adsorbed DNA
F	pulling force, orientated in z-direction
H	pitch height of DNA in the nucleosome
k_{ad}	pure adsorption energy density per wrapped length
R	histone core radius
$\overline{R}$	$\overline{R}^2 = R^2 + \frac{H^2}{4\pi^2}$
Δz	length change in the direction of the pulling force
α	DNA desorption angle
β	out of plane tilting of the spool
ε_{ads}	nucleosome adsorption energy density

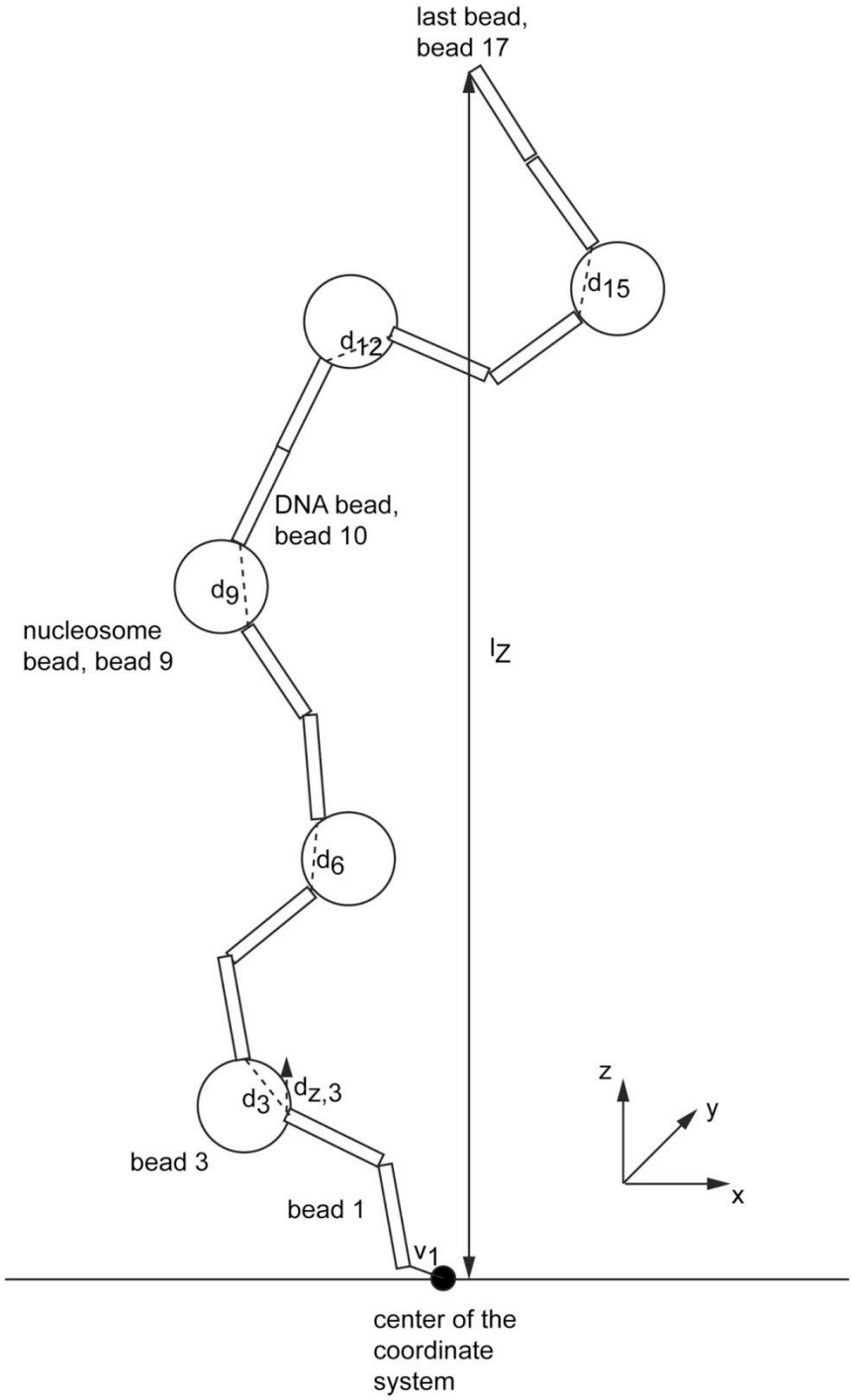

Supporting Figure S1. Scheme of pulling at a chromatin fiber. The chromatin fiber consists of nucleosome and DNA beads. It is fixed at the origin of the coordinate system with a "spring"-like linker v1 to the first DNA bead. The pulling force is applied in z–direction. Unwrapping of the DNA from the histone octamer core is accounted for in some of the simulations by an extra potential that increases the distance *d* as described in Methods.

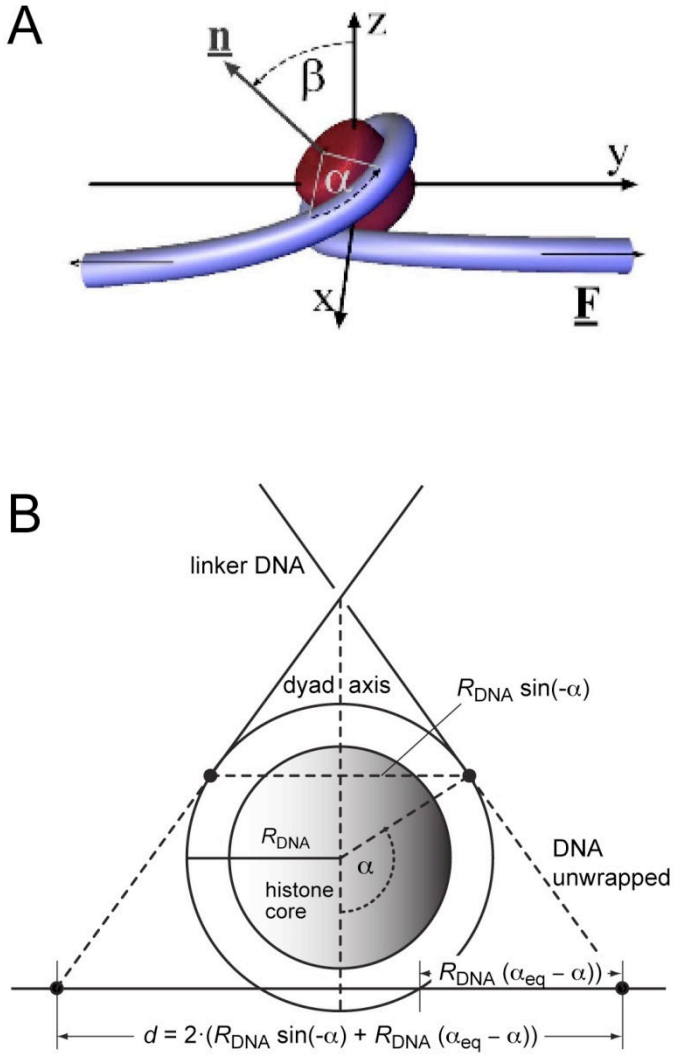

Supporting Figure S2. Parameterization of DNA unwrapping. (*A*) Definition of α and β. The image is taken from Kulić and Schiessel.[3] (*B*) Scheme to derive a relation between *d* and α. Unwrapping of DNA from the histone core changes the angle α and translates into a corresponding increase of distance *d* between the two ends of the linker DNA.

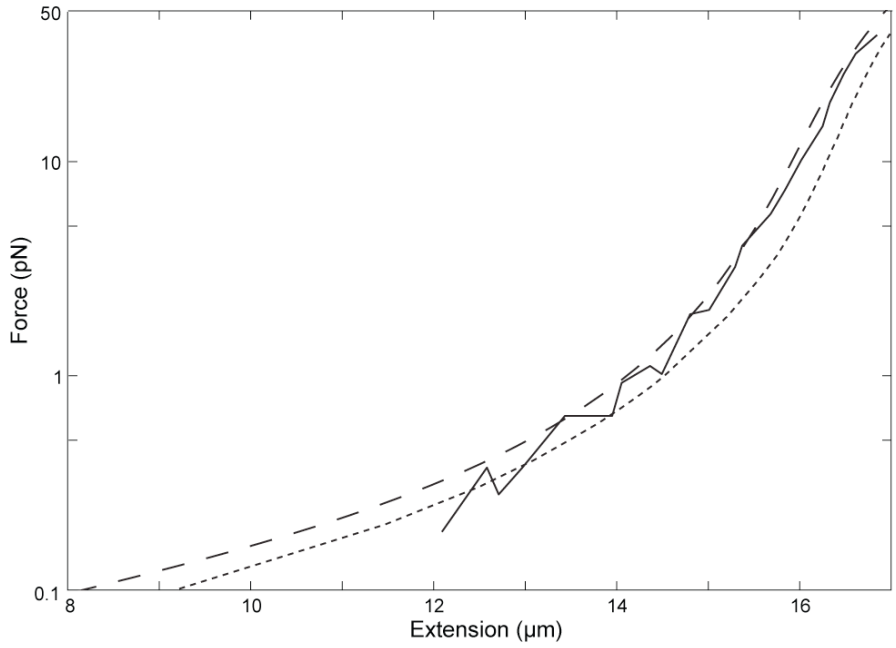

Supporting Figure S3

Force-extension curves of λ-DNA modeled with the extensible worm-like chain (WLC) polymer model (dashed line), simulated (dotted line) and experimentally measured data[4] (solid line). The DNA with a total length of 48.5 kb was represented in the simulations by 970 DNA segments (17 nm per segment). The simulations were performed with the same parameters used for chromatin fibers (Table S2 and S3). To calculate the extension x of DNA with a given contour length L_0 and persistence length P in response to a stretching force F in WLC model the following equation according[5,6] was used:

$$\frac{FP}{k_B T} = \frac{1}{4}\left(1 - \frac{x}{L_0} + \frac{F}{K_0}\right)^{-2} - \frac{1}{4} + \frac{x}{L_0} - \frac{F}{K_0}$$

The DNA stretch modulus K_0 is $1.1 \cdot 10^{-18}$ J nm as in the MC simulations, k_B is the Boltzmann constant, and T is the temperature. The DNA persistence length P = 50 nm and a contour length L_0 of λ-DNA (16.5 μm) were used. The results of the MC simulations agree well with the experimentally measured curve of Baumann et al.[4] and demonstrate that this approach is suited for the comparison with experimental data. As expected, the simulated force-extension curve touches the lower limit of the experimental curve, since the MC simulation will always calculate extensions in the thermodynamic equilibrium while the experimental curve may not always be completely equilibrated. It is noted that the absolute length of extension could be derived from the simulations. This extends the previous work of Vologodskii and Marko,[7] where shorter DNA fibers were simulated and relative changes in length were compared.

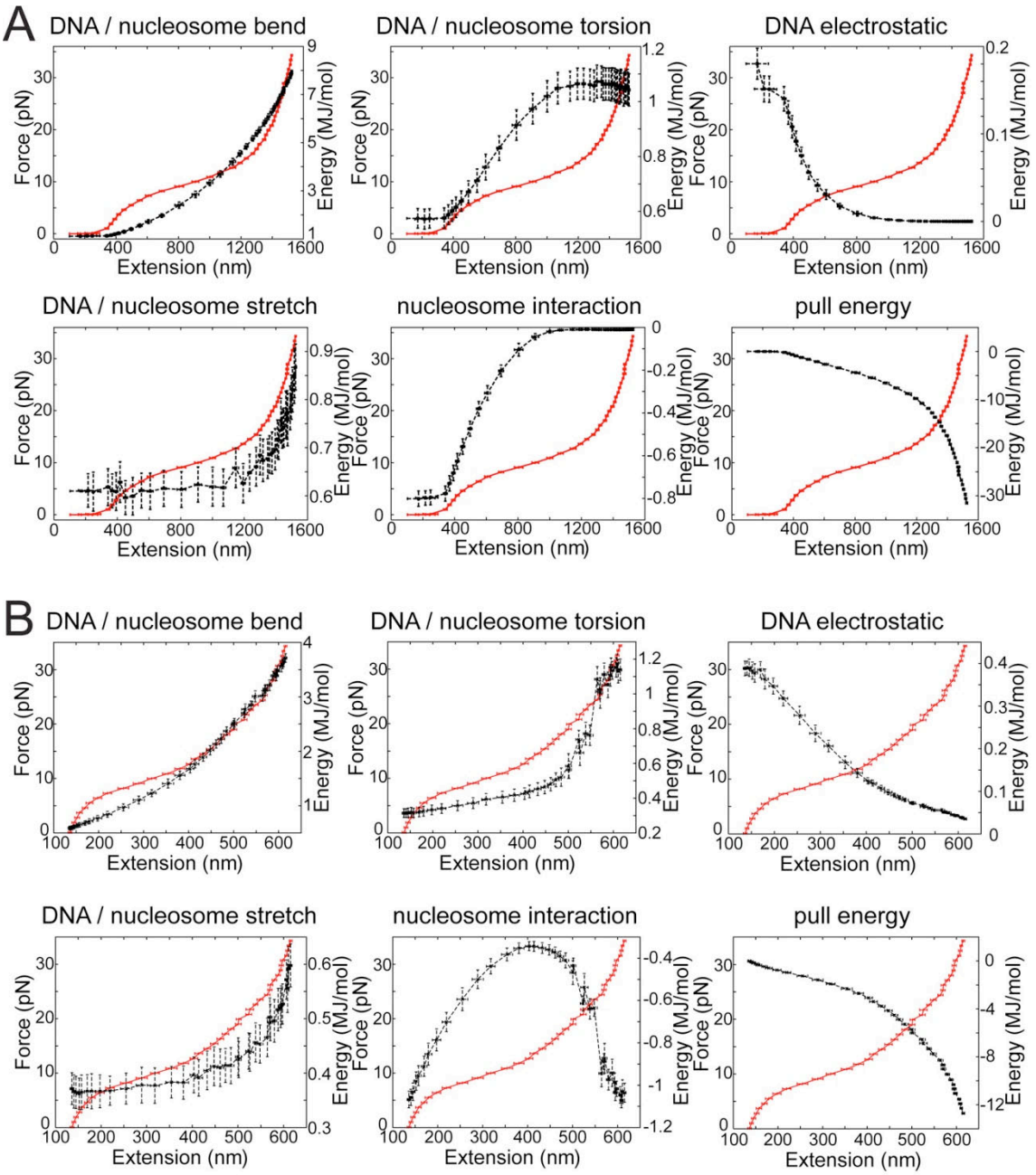

Supporting Figure S4. Comparison of the different energetic terms (black line) to the shape of the force-extension curve (red line). The energy-extension curves of DNA/nucleosome torsion, stretching and bending, electrostatics of the DNA, interaction between nucleosomes, and pulling of the fiber are shown. In case of nucleosomes, torsion, bending and stretching is related to the entry and exit point of the DNA. Simulations were conducted for a nucleosome-nucleosome interaction energy of E_{max} = 6 k_BT. (*A*) Force-extension curves and energies of a CL nucleosome geometry with 169 bp NRL. (*B*) Force-extension curves and energies of an ID nucleosome geometry with 187 bp NRL.

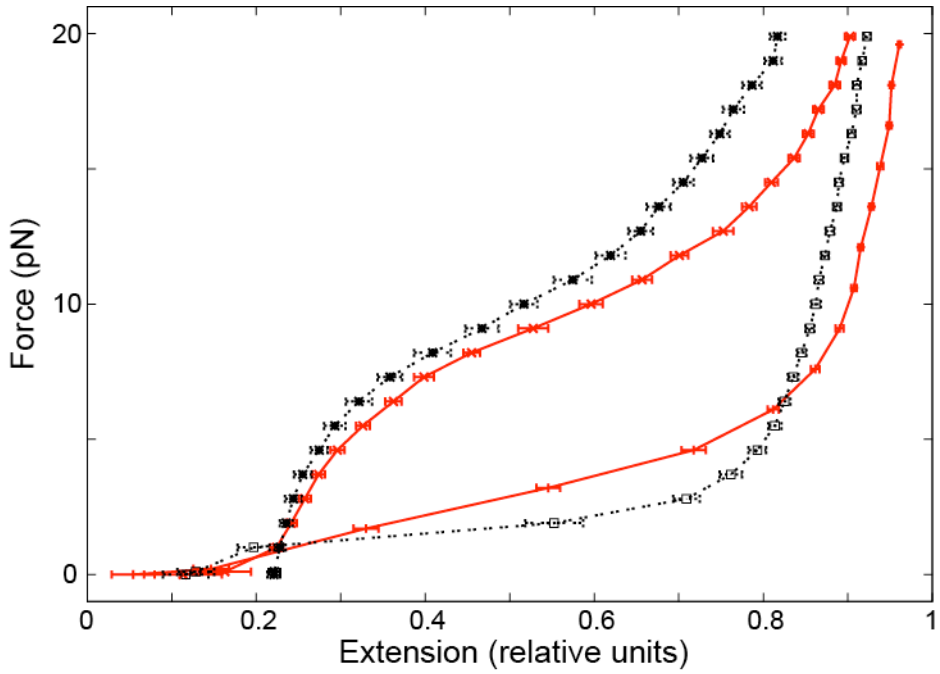

Supporting Figure S5. Comparison of simulations with different fiber geometries. Force-extension curves (plotted as relative extensions) of chromatin fibers with CL (red lines) and ID (black lines) nucleosome geometry using the same maximal nucleosome interaction energy of 6 k_BT. For the two upper curves the effective nucleosome interaction energy was ~2 k_BT. For each tested combination of NRL and nucleosome geometry a similar shaped curve with another geometry can be produced.

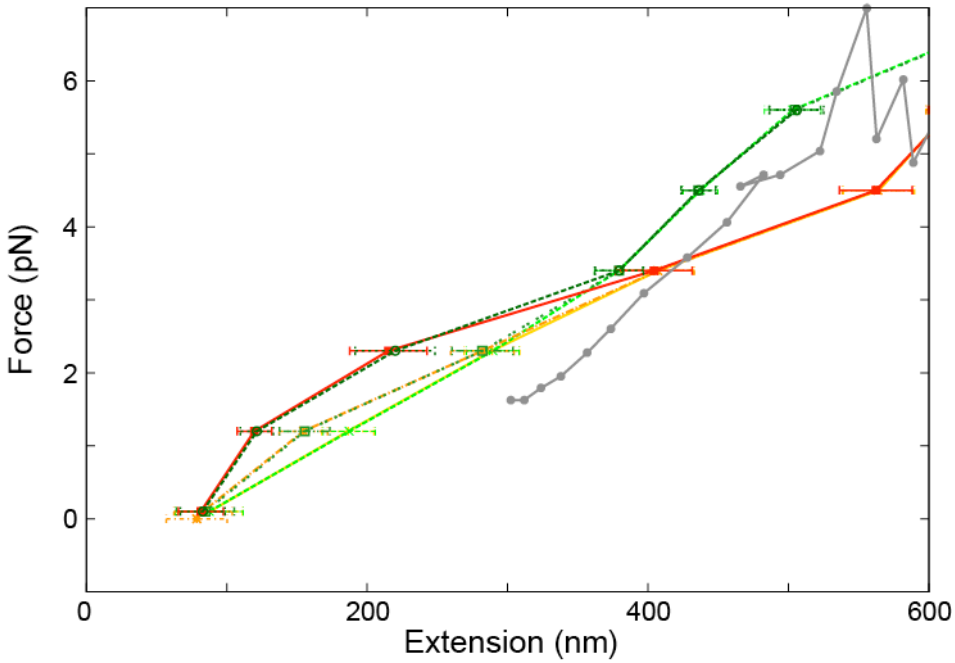

Supporting Figure S6. Nucleosome interaction energies influence the shape of the force extension curve in the beginning, E_{max} = 6 (yellow, light green), 9 (orange, forest green) and 12 (red, dark green) k_BT. The shape is later on dominated by the nucleosome unwrapping, k_{ad} = 3 (orange colors) and 4 (green colors) k_BT nm^{-1}. The experimental values from Brower-Toland et al.[8] (gray curve) are more extended than the simulated. See text for further details.

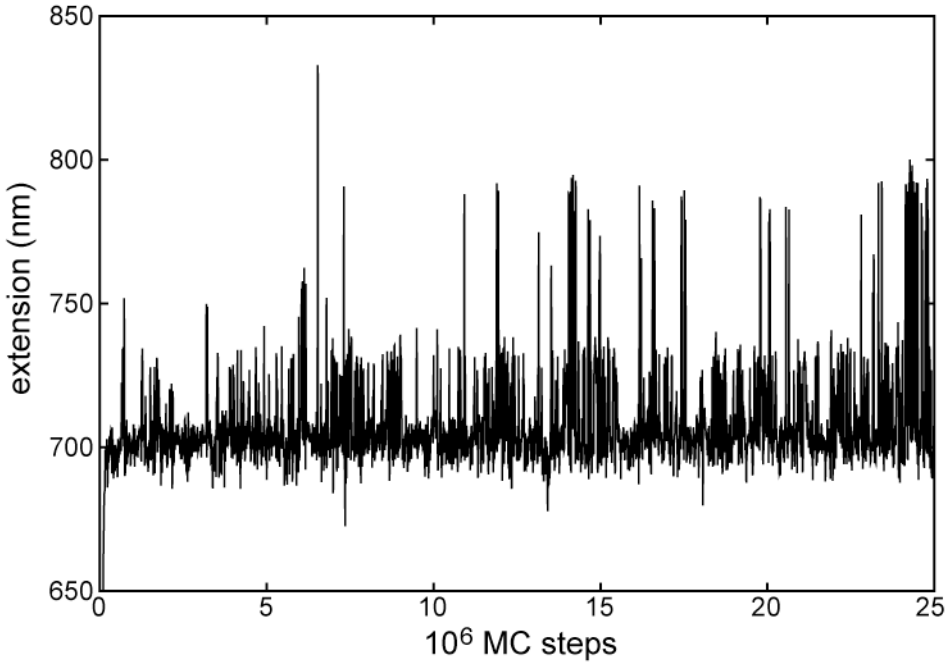

Supporting Figure S7. The evolution of the chromatin fiber extension during the MC simulations is shown. Calculations were done for a fiber with 17 nucleosomes in CL geometry, an adsorption energy k_{ad} = 4 k_BT, and an applied pulling force of 14.4 pN. In this regime the inner DNA turn of the nucleosome reversibly unwrapped, leading to an increase of the chain end-to-end length by about 25 nm/nucleosome.

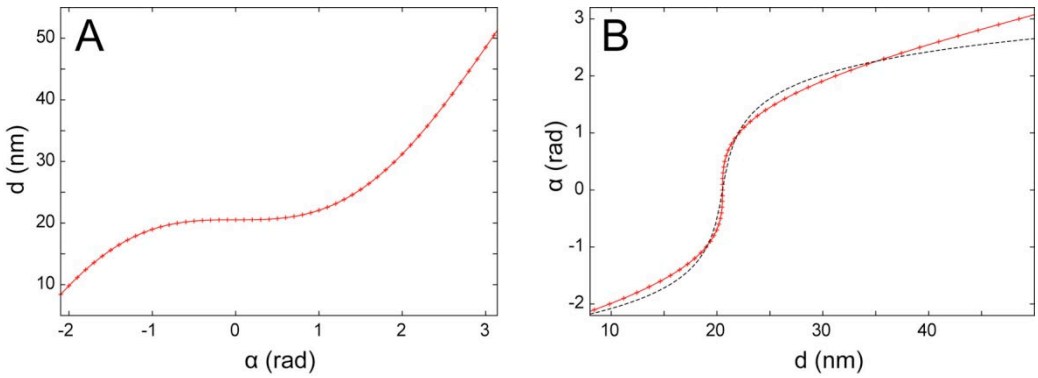

Supporting Figure S8. Connection between α and $\left|\vec{d}\right|$ of the 6–angle model as derived in the supporting text. (*A*) Equation S8 in the range relevant for nucleosome unwrapping with R_{DNA} = 4.9 nm and $\alpha_{crystal}$ = 2.1 rad. (*B*) Inverse function of eq. S8 (red) and fitted function (black) according to eq. S9 with fit parameters *f1* = -0.56, *f2* = -1.942 and *f3* = 20.52.

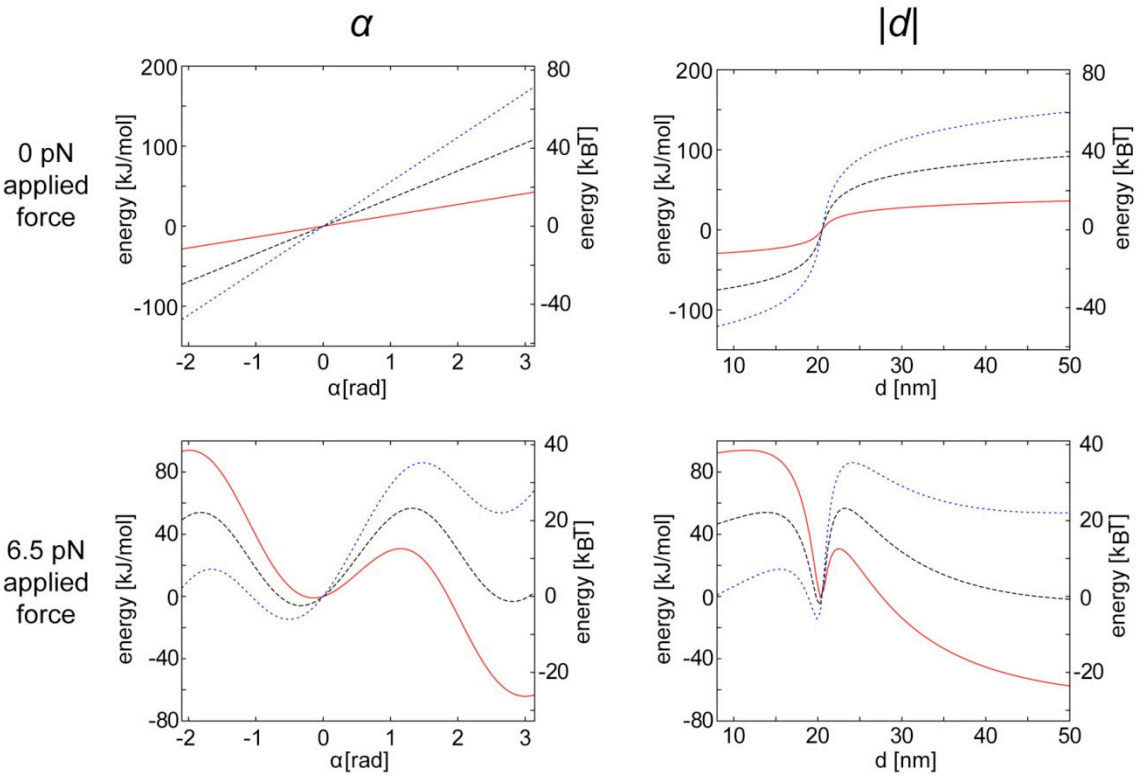

Supporting Figure S9. Comparing the unwrapping energy for pulling forces F of 0 and 6.5 pN. The complete unwrapping from 147 bp of DNA is shown as described in the supporting text. Left panel: variable *α* according to eq. S6. Right column: Equation S6 was transformed to vector *d* by using the fit function of eq. S9 from with the parameters *f1*= -0.56, *f2*= -1.942, and *f3*= 20.52. The total energy is plotted in dependence of k_{ad}, which describes the strength of the adsorption energy: k_{ad} = 2 $k_B T$ nm^{-1} (red curve); k_{ad} = 3 $k_B T$ nm^{-1} (black curve); blue curve: k_{ad} = 4 $k_B T$ nm^{-1}. A = 50 k_BT nm and R = 4.3 nm were used.

Supporting Text S1

Implementation of the DNA unwrapping potential from the histone core

Theoretical description of nucleosome unwrapping potential

The nucleosome unwrapping potential introduced by Kulić and Schiessel[3,9] was implemented in the Monte Carlo simulation of Chromatin *MC2*[1,10,11] as described below. A detailed description of other aspects of *MC2* software can be found in the supporting material of reference.[11] The unwrapping energy of a nucleosome can be calculated with Equation SS1, according to Kulić and Schiessel.[3]

$$E_{\mathrm{uw}} = E_{\mathrm{bend}} + 2R\varepsilon_{\mathrm{ads}}\alpha - 2F\Delta z \tag{S1}$$

The parameters used in the potential are listed in Table S4. The first term is the DNA bending energy, the second term is the adsorption energy, and the third term describes the gain in the potential energy for stretching the DNA ends by a distance 2Δ*z* at a given force *F*. Applying linear elasticity theory and elementary geometry E_{uw} can be dissected into the following three terms[3]:

$$E_{\mathrm{uw}}(\alpha,\beta) = E_{\mathrm{comp}}(\alpha) + E_{\mathrm{geom}}(\alpha,\beta) + E_{\mathrm{stiff}}(\alpha,\beta) \tag{S2}$$

with:

$$E_{\mathrm{comp}}(\alpha) = 2R\cdot(\varepsilon_{\mathrm{a}} - F)\cdot\alpha \tag{S3}$$

$$E_{\mathrm{geom}}(\alpha,\beta) = 2FR\cdot\left(\cos(\beta)\cdot\sin(\alpha) - \frac{\pi-\alpha}{2\pi R}\cdot H\cdot\sin(\beta)\right) \tag{S4}$$

$$E_{\mathrm{stiff}}(\alpha,\beta) = 8\cdot\sqrt{AF}\cdot\left(1-\sqrt{\frac{1+\frac{R}{\overline{R}}\cdot\cos(\beta)\cdot\cos(\alpha)+\frac{H}{2\pi\overline{R}}\cdot\sin(\beta)}{2}}\right) \tag{S5}$$

Unwrapping of the nucleosome is described in this potential by the two variables α and β (see Figure S2 A). The degree of DNA adsorption is described by the desorption angle α which is defined as zero for one full turn wrapped around the histone octamer protein core (see Figure S2 B). An additional angle β accounts for the out–of–plane tilting of the spool and describes the rotation of the nucleosome around its dyad–axis.[12]

A simplified version of the potential for a flat spool with $R \gg H$ is presented by Kulić and Schiessel.[9] Based on analysis of the energy landscape the additional approximation $\alpha = \beta$ is introduced.

$$E_{\mathrm{uw}}(\alpha) \approx \quad 2R \cdot \left(k_{\mathrm{ad}} - \frac{A}{2R^2} - F\right) \cdot \alpha + 2FR \cdot \cos(\alpha) \cdot \sin(\alpha) + 8 \cdot \sqrt{AF} \cdot \left(1 - \sqrt{\frac{1+\cos(\alpha)^2}{2}}\right) \tag{S6}$$

The nucleosome adsorption energy density, $\varepsilon_{\mathrm{ads}}$, and pure adsorption energy density per wrapped length, k_{ad}, are connected by the Equation:

$$\varepsilon_{\mathrm{ads}} = k_{\mathrm{ad}} - \frac{A}{2R^2} \tag{S7}$$

Expressing α and β via parameters of the six–angle model

In the six–angle model for chromatin fibers[10] $\vec{d}$ is defined as vector between the points where the DNA enters and leaves the nucleosome (see Figure S2 B). For nucleosomes without linker histone $\vec{d}$ is derived from information of the nucleosome crystal structure,[12] where no pulling force is applied. To account for DNA unwrapping $\left|\vec{d}\right|$ is computed as

$$|\vec{d}| = 2R_{\mathrm{DNA+core}} \cdot \sin(\alpha) + 2R_{\mathrm{DNA}} \cdot (\alpha_{\mathrm{eq}} + \alpha) \tag{S8}$$

The radius of the histone core together with the radius of the wrapped DNA $R_{\mathrm{DNA+core}}$ is about 4.9 *nm*. The parameter α_{eq} is the value of the angle α in the relaxed nucleosome, measured in the crystal structure.[12] It is 120°. Computing the unwrapping energy according to Equation S6 needs to compute α from a given $\left|\vec{d}\right|$. Therefore Equation S9 was fitted to the "inverted" graph of Equation S8 (see Figure S8). In the relevant range Equation S8 is monotone. Therefore the map to an inverse function is unique. The best fit parameters were $f1 = -0.56$, $f2 = -1.942$, and $f3 = 20.52$.

$$\alpha(|\vec{d}|) = f1 \cdot \operatorname{arcsinh}\left(f2 \cdot (|\vec{d}| - f3)\right) \tag{S9}$$

The adsorption energy density has a strong influence on the unwrapping potential. Figure S9 shows the unwrapping energy E_{uw} according to Equation S6 for different values of k_{ad}. Due to the nonlinear transformation from α to $\left|\vec{d}\right|$, the shape of the curves depends on the input

parameter *α* or $\left|\vec{d}\right|$, but the number and relative position of the minima and maxima remain the same.

Implementation into the *MC2* software

In the *MC2* simulation software the pulling force *F* is applied in z–direction of the global coordinate system. The gain of potential energy by pulling at one fiber end while the other is fixed $E_{\text{pull,fiber}}$ is calculated as described in Equation S10 (see also Figure S1).

$$E_{\text{pull,fiber}} = k_{\text{hold}} \cdot |\vec{v}_1|^2 - F_{\text{pull}} \cdot l_{\text{z}} \tag{S10}$$

In Equation S10 k_{hold} determines the strength, with which the first “bead” of the chromatin chain is attached to the origin of the coordinate system. This represents the attaching of the fiber at a cover–slip in force–extension experiments (see Figure S1). $\left|\overrightarrow{v_1}\right|$ is the distance of the first “bead” to the origin of the coordinate system or the point of fixation. The fiber–ground adhesion module k_{hold} = 333 *kJ/(mol nm²)* has been chosen such that the first bead does not move more than ~0.3 *nm* during a Monte Carlo simulation. F_{pull} is the applied pulling force and $l_{\text{Z}} = \vec{l} \cdot \hat{u}_{\text{Z}}$ is the dot product of the vector from the origin to the last “bead” with the unit vector in z–direction.

The rotation of the nucleosome is represented by changes in *β* and takes place when the first 0.67 turns of DNA are unwrapped. In this state the interactions between the nucleosomes are weakened and the influence of the orientation of the nucleosome in the context of the fiber is low. Therefore, in the *MC2* simulation the approximation *α* = *β* can be used.

Equation S10 is an efficient approach to calculate the pulling energy potential of the complete fiber. Since the unwrapping potential also accounts for the gain of potential energy by pulling DNA from the histone core, this term has to be considered. Based on Equation S1 the potential energy gain pulling out the DNA can be subtracted from the unwrapping potential Equation S6. Therefore Equation S6 is modified in *MC2* to:

$$\begin{aligned} E_{\text{uw}}(\vec{d}) = \quad & 2R \cdot \left(k_{\text{ad}} - \frac{A}{2R^2} - F\right) \cdot \alpha + 2FR \cdot \cos(\alpha) \cdot \sin(\alpha) + \\ & 8 \cdot \sqrt{AF} \cdot \left(1 - \sqrt{\frac{1+\cos(\alpha)^2}{2}}\right) + F \cdot \frac{d_{\text{z}}}{|\vec{d}|} \cdot \Delta|\vec{d}| \end{aligned} \tag{S11}$$

The parameter α is calculated according to Equation S9. For the simulations $A = 50\ k_BT\ nm$ and $R = 4.3\ nm$ were used according to Kulić and Schiessel.[3] When the nucleosome is completely unwrapped the same potential as for the linker DNA is used in case of complete further elongation (see Wedemann and Langowski[2]). In case of wrapping more than 1.67 turns of DNA on the histone core, the potential developed for nucleosomes without unwrapping will be used.[2]

References

1. Stehr, R.; Kepper, N.; Rippe, K.; Wedemann, G. Biophys J 2008, 95, 3677-3691.
2. Wedemann, G.; Langowski, J. Biophys J 2002, 82, 2847-2859.
3. Kulić, I. M.; Schiessel, H. Phys Rev Lett 2004, 92, 228101.
4. Baumann, C. G.; Smith, S. B.; Bloomfield, V. A.; Bustamante, C. Proc Natl Acad Sci USA 1997, 94, 6185-6190.
5. Marko, J. F.; Siggia, E. D. Macromolecules 1995, 28, 8759-8770.
6. Odijk, T. Macromolecules 1995, 28, 7016-7018.
7. Vologodskii, A. V.; Marko, J. F. Biophys J 1997, 73, 123-132.
8. Brower-Toland, B. D.; Smith, C. L.; Yeh, R. C.; Lis, J. T.; Peterson, C. L.; Wang, M. D. Proc Natl Acad Sci USA 2002, 99, 1960-1965.
9. Kulic, I. M.; Schiessel, H. In DNA interactions with polymers and surfactants; Dias, R. S.; Lindman, B., Eds.; Wiley: London, 2008, p 173-208.
10. Kepper, N.; Foethke, D.; Stehr, R.; Wedemann, G.; Rippe, K. Biophys J 2008, 95, 3692-3705.
11. Stehr, R., Schöpflin, R., Ettig, R., Kepper, N., Rippe, K. & Wedemann, G. Biophys J 2010, 98, 1028 - 1037.
12. Davey, C. A.; Sargent, D. F.; Luger, K.; Maeder, A. W.; Richmond, T. J. J Mol Biol 2002, 319, 1097-1113.